Longitudinal, Deep, and Network Biomarkers: Parenclitic and Synolitic Network Analysis

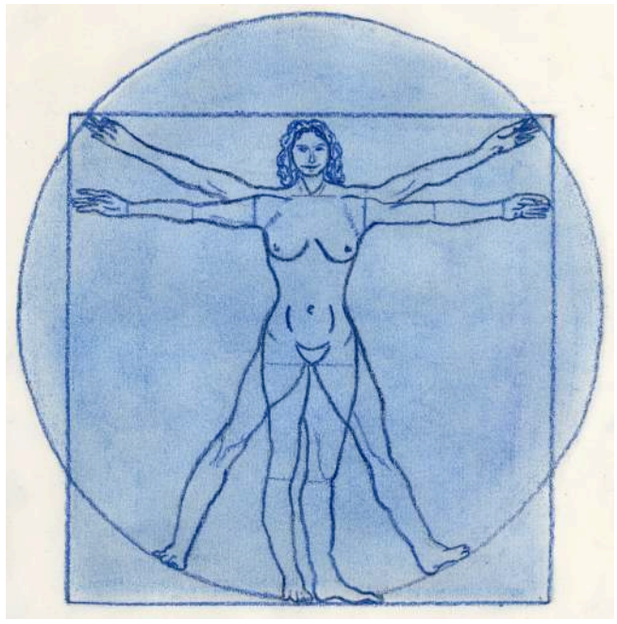

Alexey Zaikin

Institute for Women's Health and Department of Mathematics
University College London

www.zaikinlab.com

alexey.zaikin@ucl.ac.uk

How to Construct Network Biomarkers, if There is No Network??

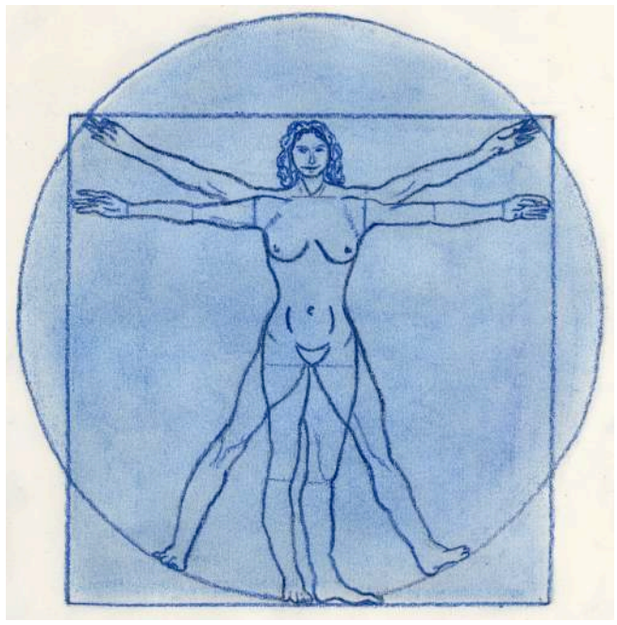

Alexey Zaikin

Institute for Women's Health and Department of Mathematics
University College London

www.zaikinlab.com

alexey.zaikin@ucl.ac.uk

frontiers
in Aging Neuroscience

REVIEW
published: 25 May 2020
doi: 10.3389/fnagi.2020.00136

2020

The Human Body as a Super Network: Digital Methods to Analyze the Propagation of Aging

Harry J. Whitwell[1], Maria Giulia Bacalini[2], Oleg Blyuss[3,4], Shangbin Chen[5], Paolo Garagnani[6], Susan Yu Gordleeva[7], Sarika Jalan[8,9], Mikhail Ivanchenko[10], Oleg Kanakov[7], Valentina Kustikova[10], Ines P. Mariño[11], Iosif Meyerov[10], Ekkehard Ullner[12], Claudio Franceschi[7,10] and Alexey Zaikin[4,10,13]**

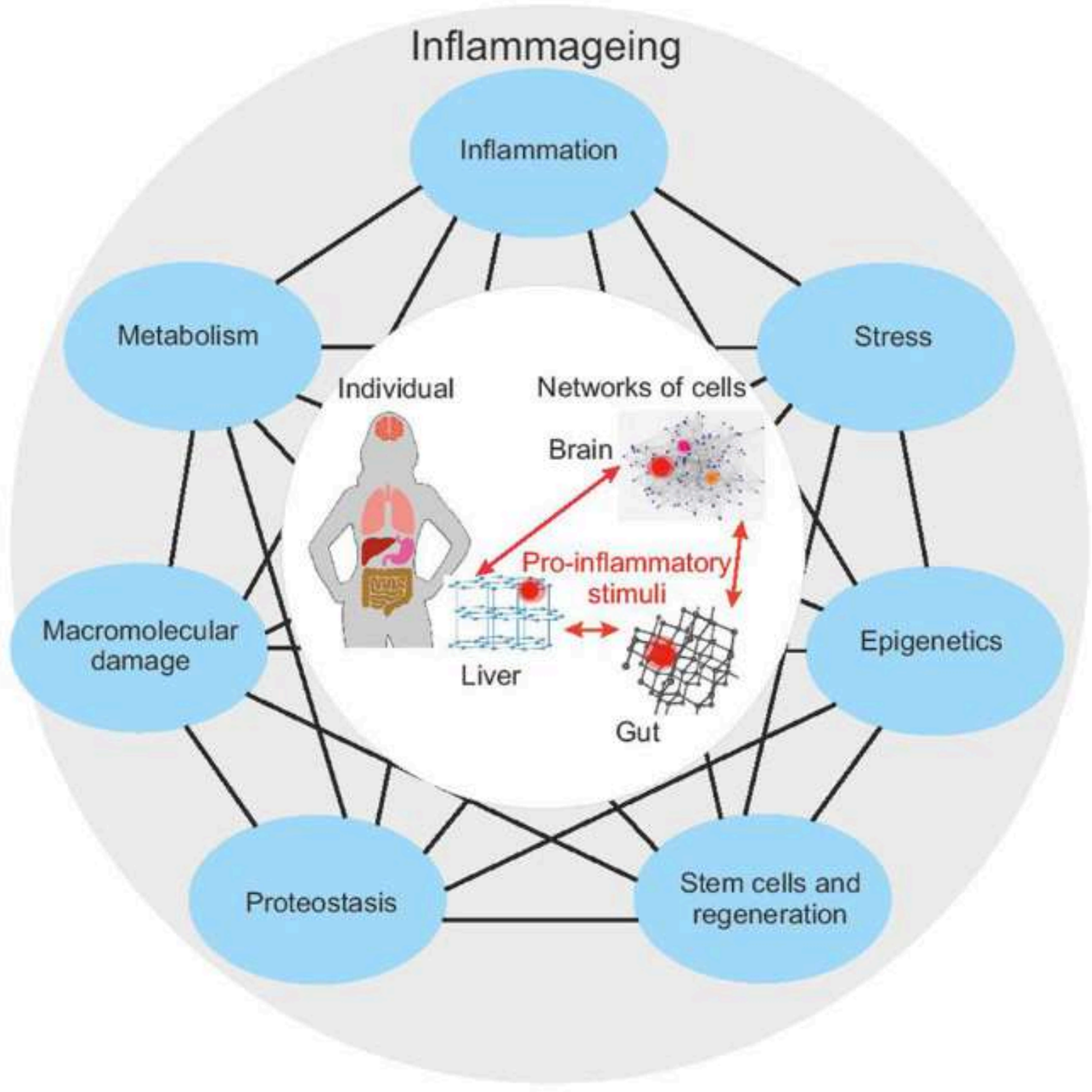

Huge amount of -Omic Information: Genome, Chromatome, Methylome, Transcriptome, Proteome

OM&P

MAMMALIAN BRAIN AS A NETWORK OF NETWORKS

Veronika Samborska [1], Susanna Gordleeva [2], Ekkehard Ullner [3], Albina Lebedeva [2], Viktor Kazantsev [2], Mikhail Ivanchenko [2] and Alexey Zaikin [2,4]

Search for Network, Longitudinal and Deep Learning Biomarkers

Multi-omic data: Genetic, Epigenetic and Proteomic

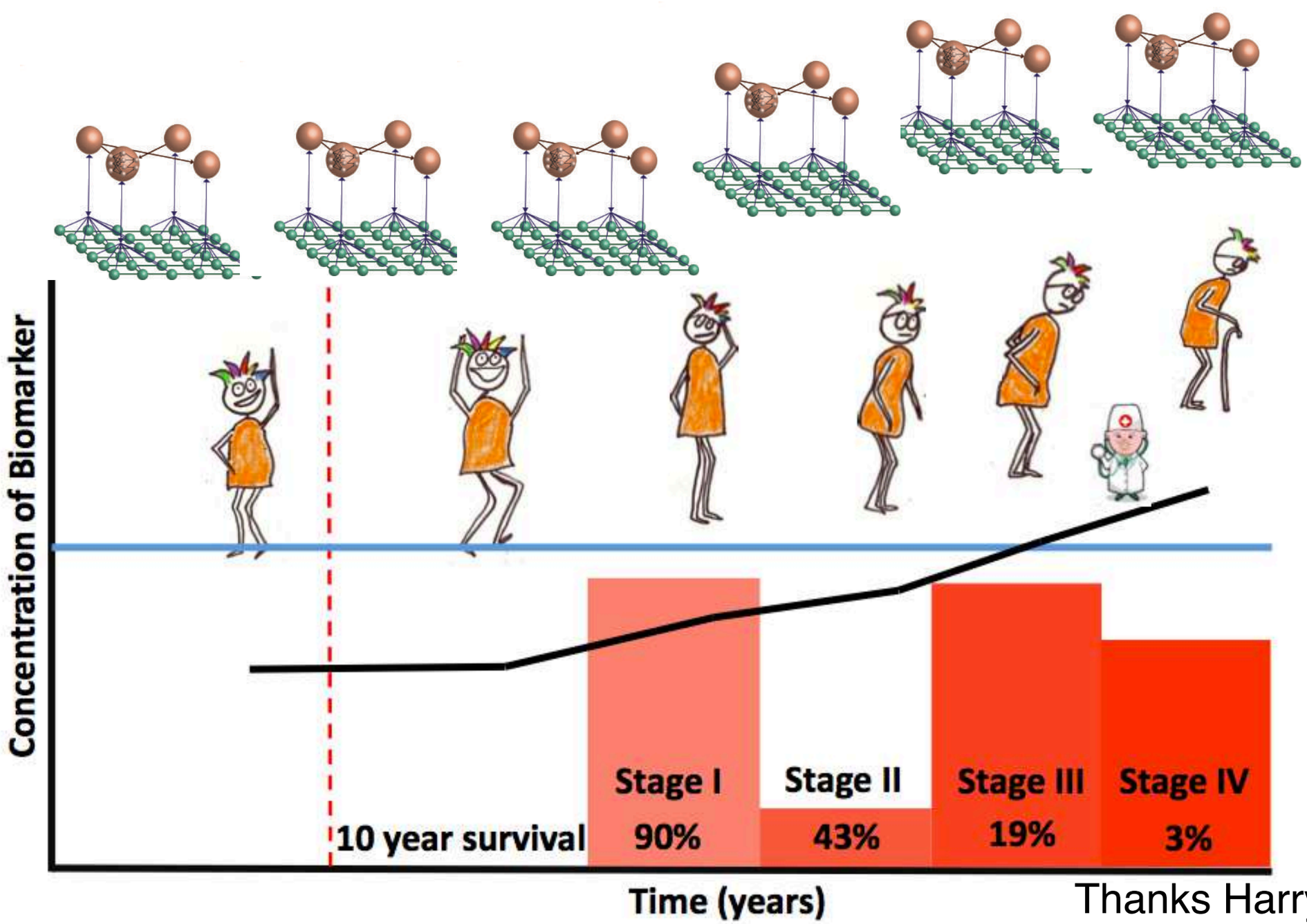

Thanks Harry for picture

Constructing network biomarkers

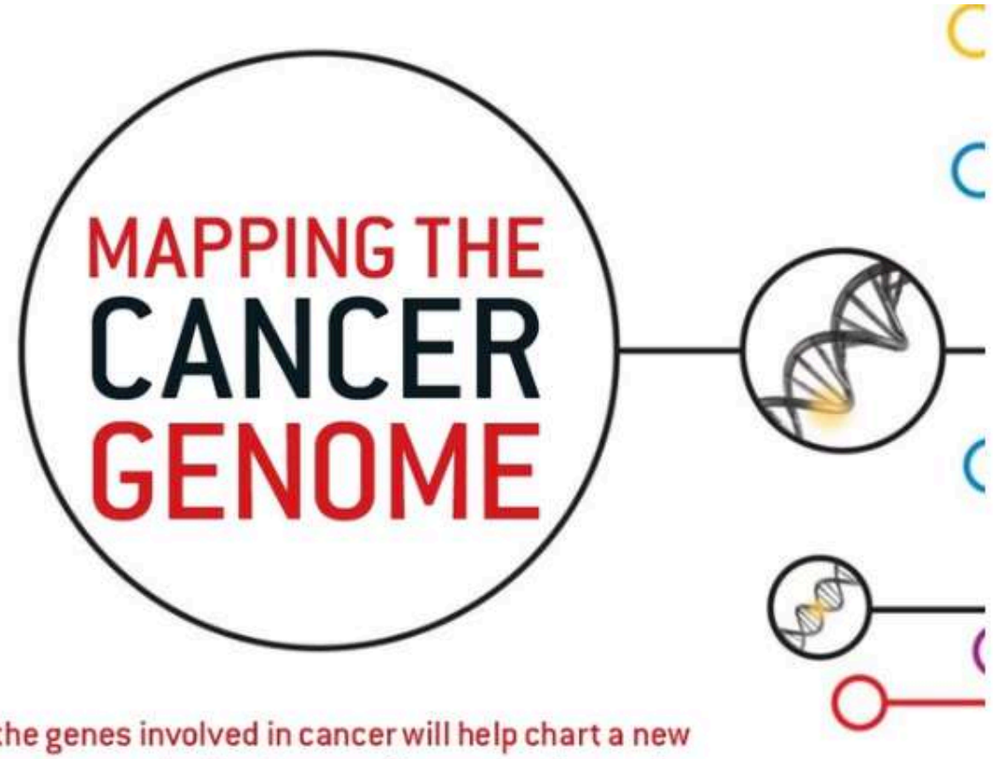

Scientific American
Vol. 296, No. 3 (MARCH 2007), pp. 50-57 (8 pages)

Pinpointing the genes involved in cancer will help chart a new course across the complex landscape of human malignancies

By Francis S. Collins and Anna D. Barker

"One difficulty in interpreting this data for defining clinically useful information is that multiple different changes may be responsible for the onset of a disease, as exemplified by the efforts of The Cancer Genome Atlas project"

Solution: topological analysis of networks

Global Genetic Landscape Of The Cell (IMAGE)

UNIVERSITY OF TORONTO

Heterogeneity

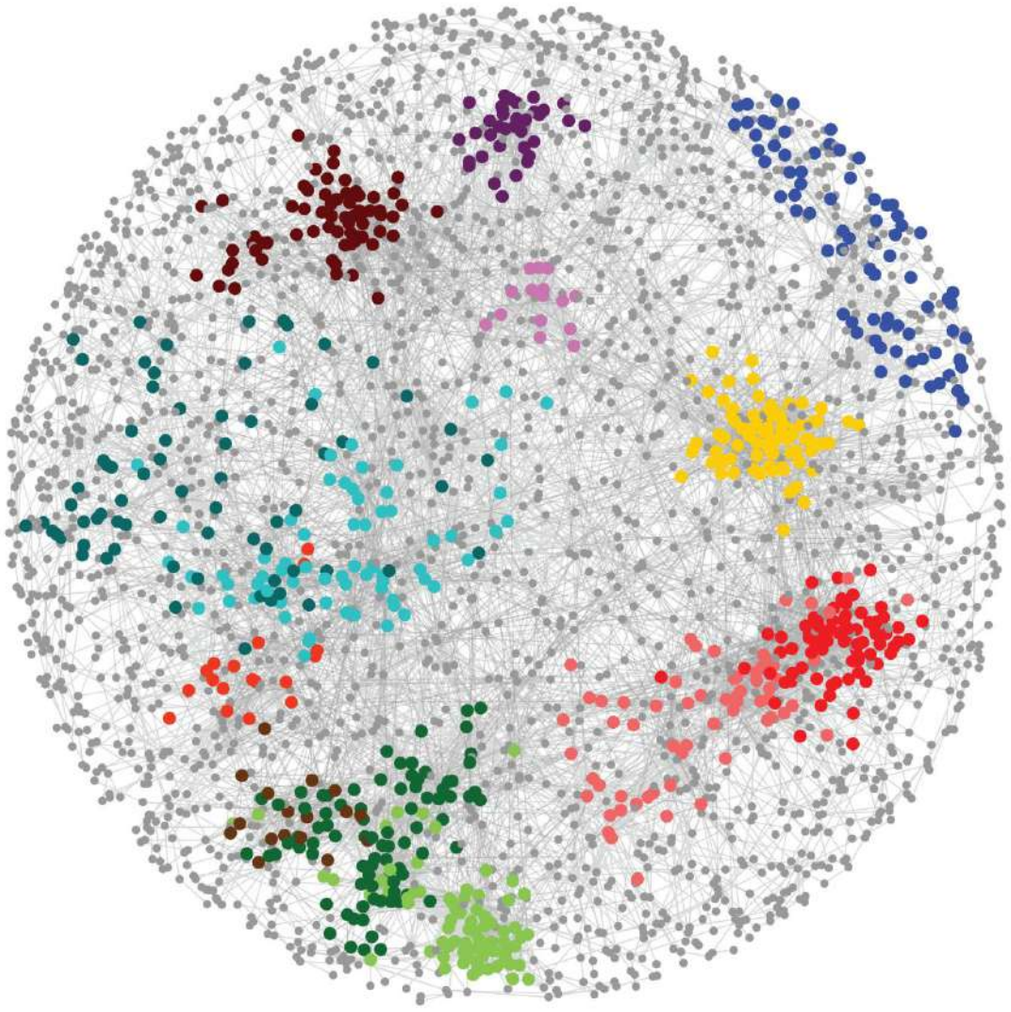

Schizophrenia Gene Networks Found, with Link to Autism

November 11, 2012

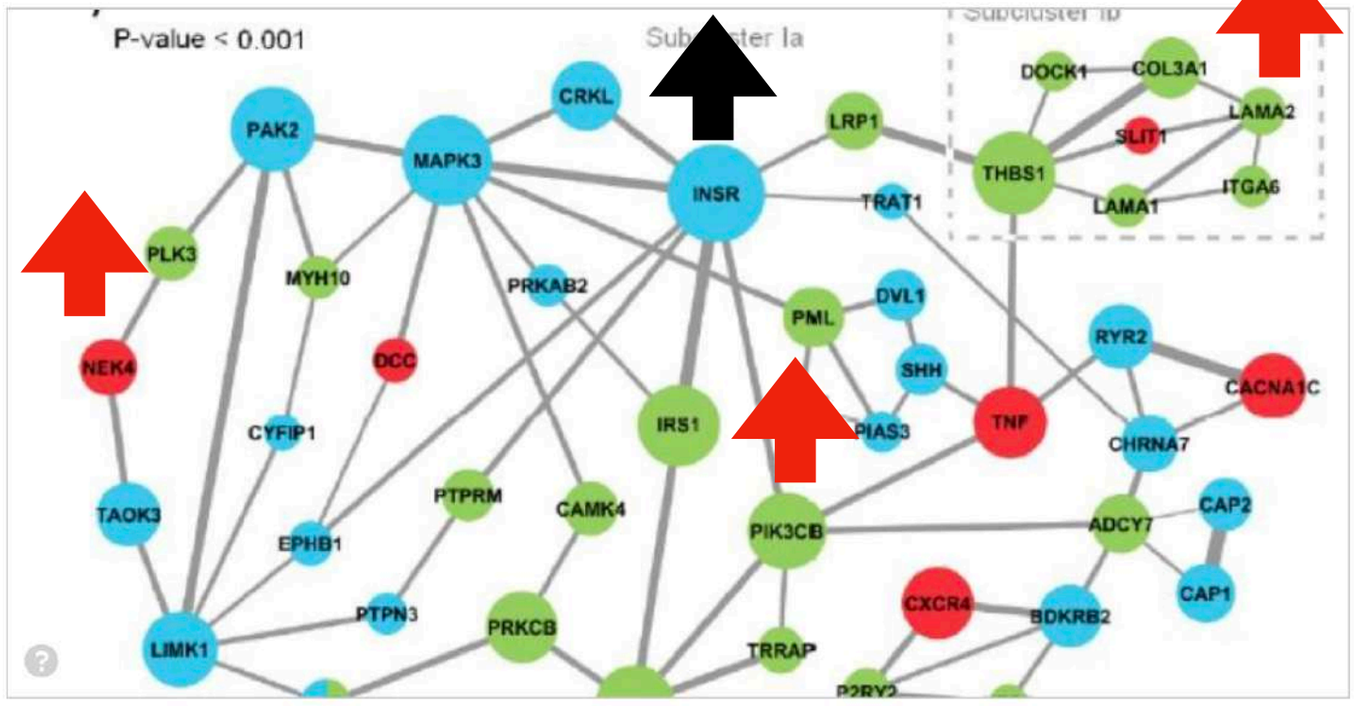

Solution: topological analysis of networks

How to construct a network if links are unknown??

Available online at www.sciencedirect.com

ScienceDirect

Physics of Life Reviews 37 (2021) 17–64

PHYSICS of LIFE reviews

www.elsevier.com/locate/plrev

Correlation graphs

Review

Dynamic and thermodynamic models of adaptation

A.N. Gorban [a,b,*], T.A. Tyukina [a], L.I. Pokidysheva [c], E.V. Smirnova [c]

Available online at www.sciencedirect.com

ScienceDirect

Physics of Life Reviews 38 (2021) 120–123

PHYSICS of LIFE reviews

www.elsevier.com/locate/plrev

Comment

Ensemble of correlation, parenclitic and synolitic graphs as a tool to detect universal changes in complex biological systems Comment on "Dynamic and thermodynamic models of adaptation" by A.N. Gorban et al.

Tatiana Nazarenko [a], Oleg Blyuss [a,b,e,g], Harry Whitwell [c,d,e,f], Alexey Zaikin [a,e,f,*]

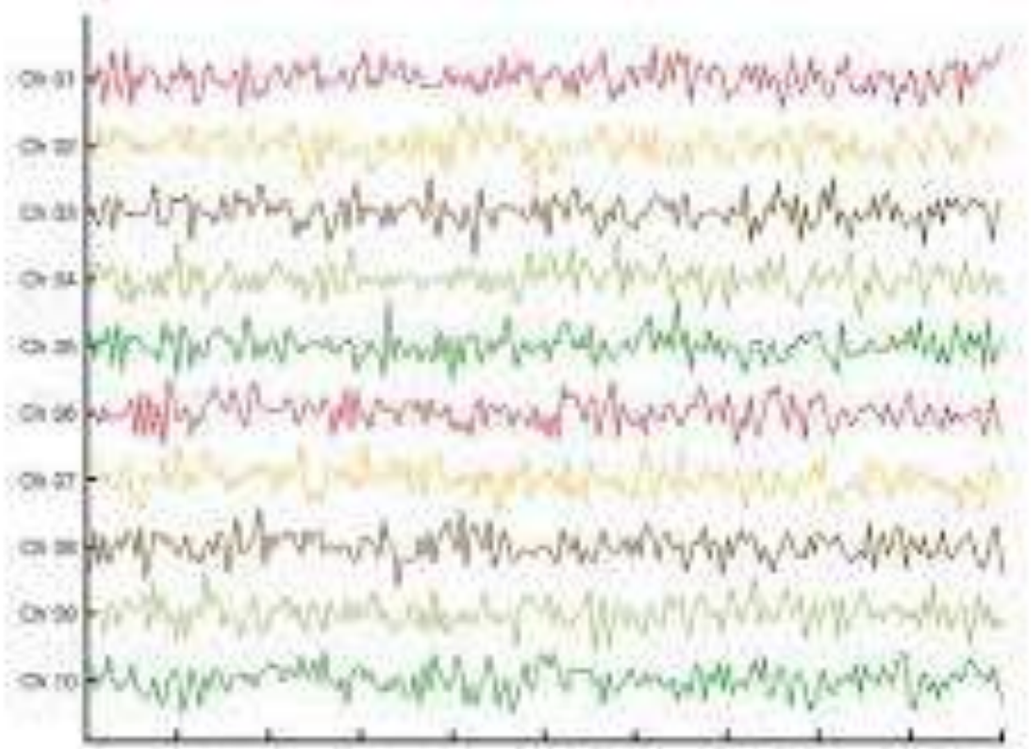

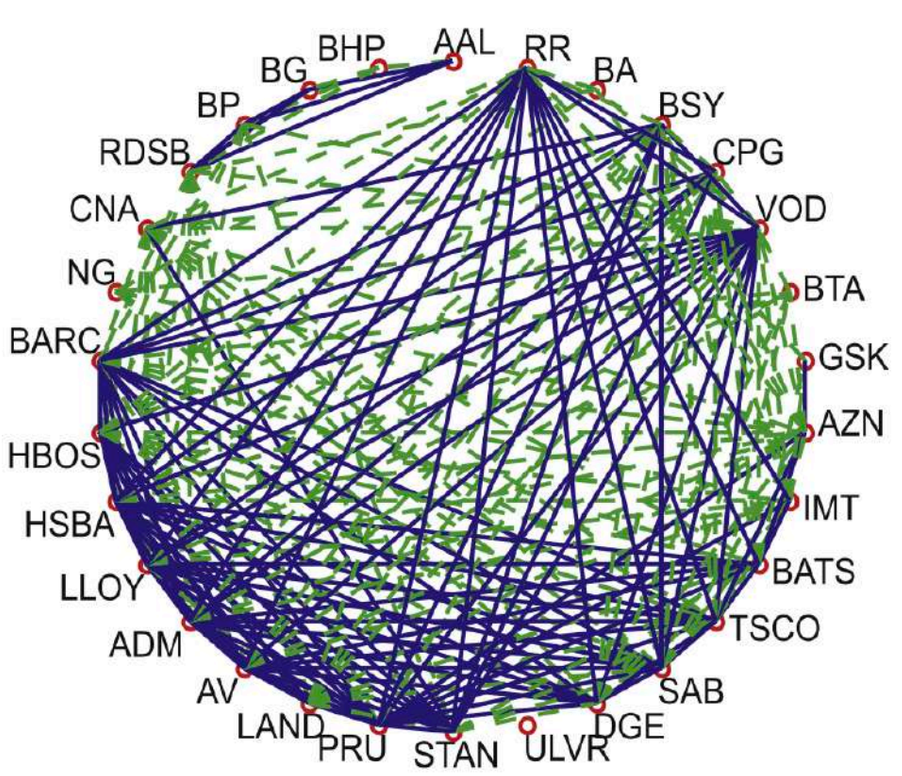

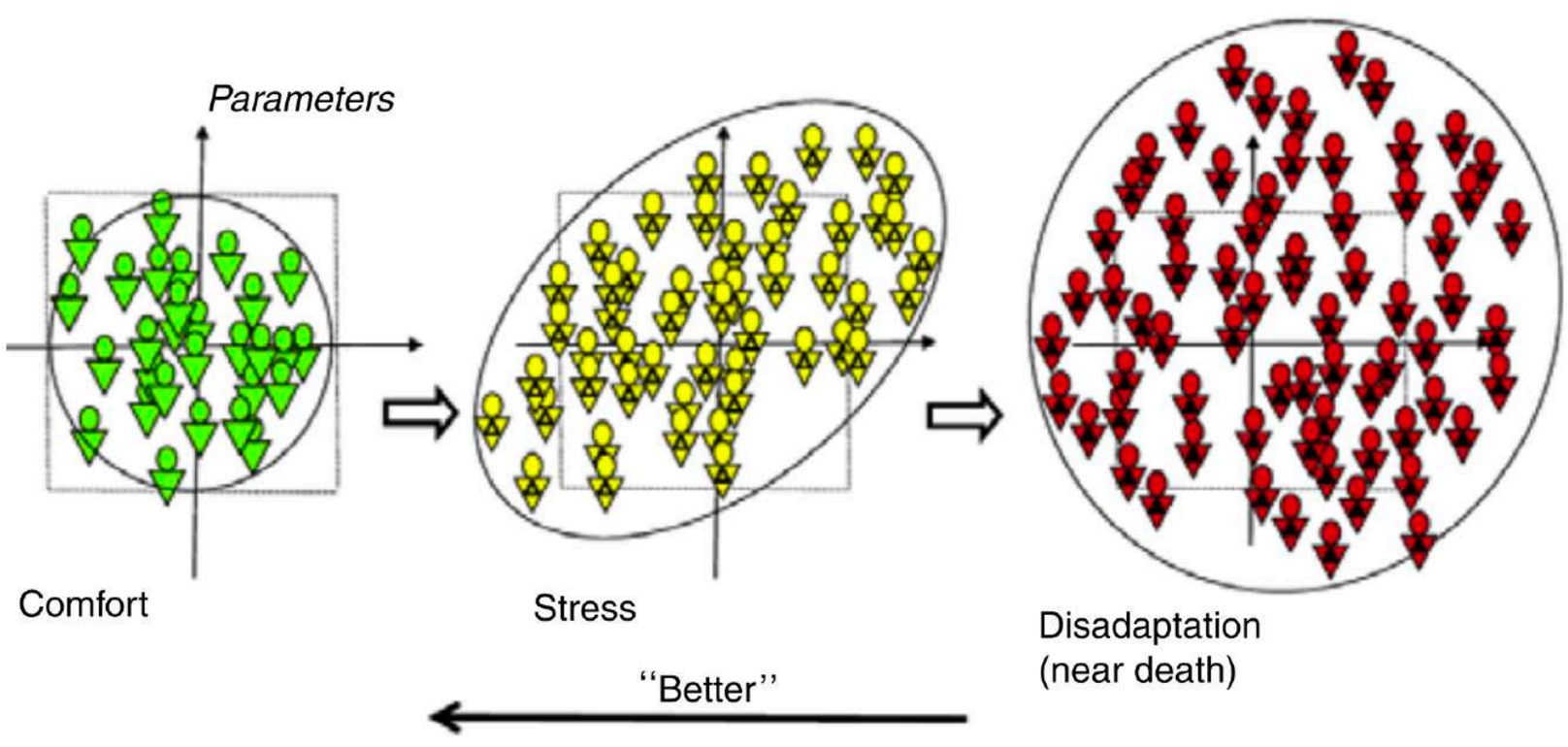

Fig. 1. Correlations and variance in crisis. The typical picture: *Cor* ↑; *Var* ↑ — stress; *Cor* ↓; *Var* ↓ — recovering; *Cor* ↓; *Var* ↑ — approaching the disadaptation catastrophe after the bottom of the crisis. In this schematic picture, axes correspond to attributes, normalized to the unite variance in the comfort state.

DNA Methylation Analysis

OPEN ACCESS Freely available online

PLOS ONE

Corruption of the Intra-Gene DNA Methylation Architecture Is a Hallmark of Cancer

Thomas E. Bartlett[1,2], Alexey Zaikin[2], Sofia C. Olhede[1,3], James West[1,4], Andrew E. Teschendorff[4], Martin Widschwendter[5]*

July 2013 | Volume 8 | Issue 7 | e68285

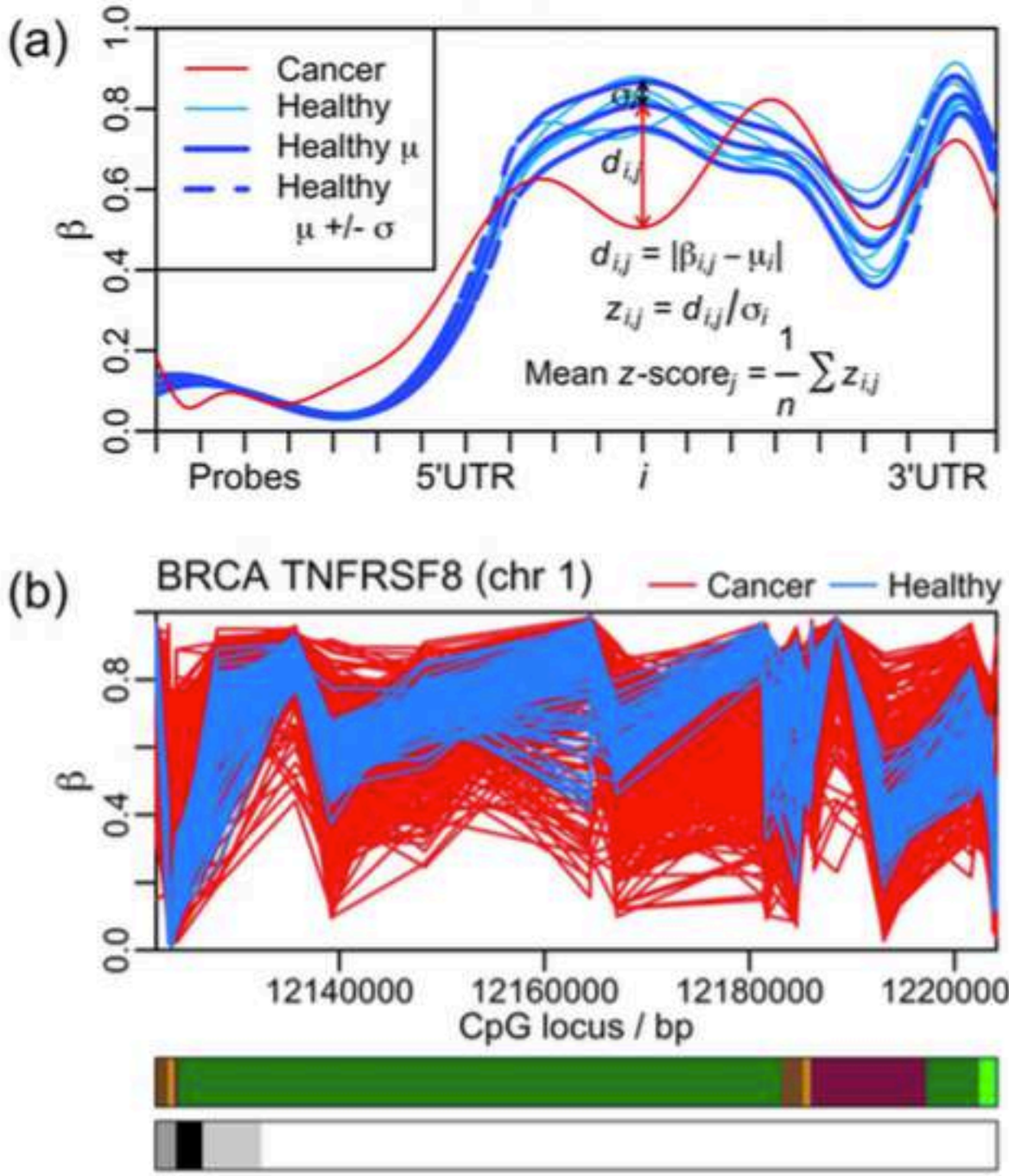

DNA Methylation

OPEN ACCESS January 2014 | Volume 9 | Issue 1 | e84573 PLOS ONE

A DNA Methylation Network Interaction Measure, and Detection of Network Oncomarkers

Thomas E. Bartlett[1,3]*, Sofia C. Olhede[2,3], Alexey Zaikin[1]

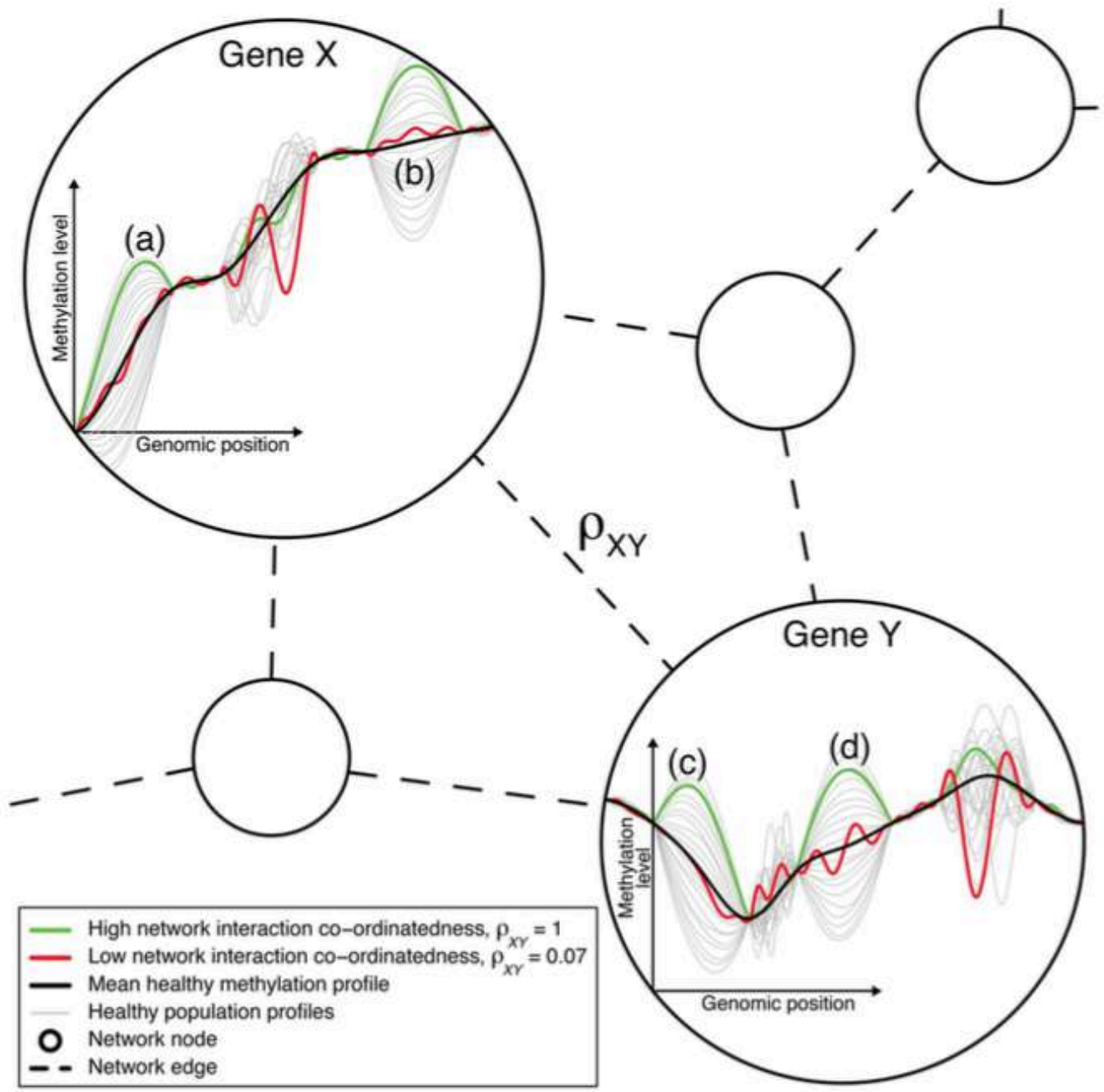

Figure 1. The DNA methylation network interaction measure. A combination of the variation of the healthy methylation profiles in regions (a) and (b) of gene X explains well/is well-explained by a combination of the variation of the healthy methylation profiles in regions (c) and (d) of gene Y. The green cancer sample varies by a large amount about the mean methylation profile and in a typical way in these regions in both genes. Hence, the green sample corresponds to a high level of network interaction co-ordinatedness, as measured by the DNA methylation network interaction measure, $\rho_{XY} = 1$. The variation in the other regions of these genes do not well-explain each other, and so the red sample, which varies by a large amount in these other regions and varies less and in an atypical way in regions (a)–(d), corresponds to a low level of network interaction co-ordinatedness, $\rho_{XY} = 0.07$. Genes X and Y are likely to have different numbers of methylation measurement locations (i.e., variables X and Y are of different dimension). The ordering of the measurement locations has no influence on the calculation of ρ, as long as the ordering is consistent across samples.

DNA Methylation Analysis

January 2014 | Volume 9 | Issue 1 | e84573

PLOS ONE

A DNA Methylation Network Interaction Measure, and Detection of Network Oncomarkers

Thomas E. Bartlett[1,3]*, Sofia C. Olhede[2,3], Alexey Zaikin[1]

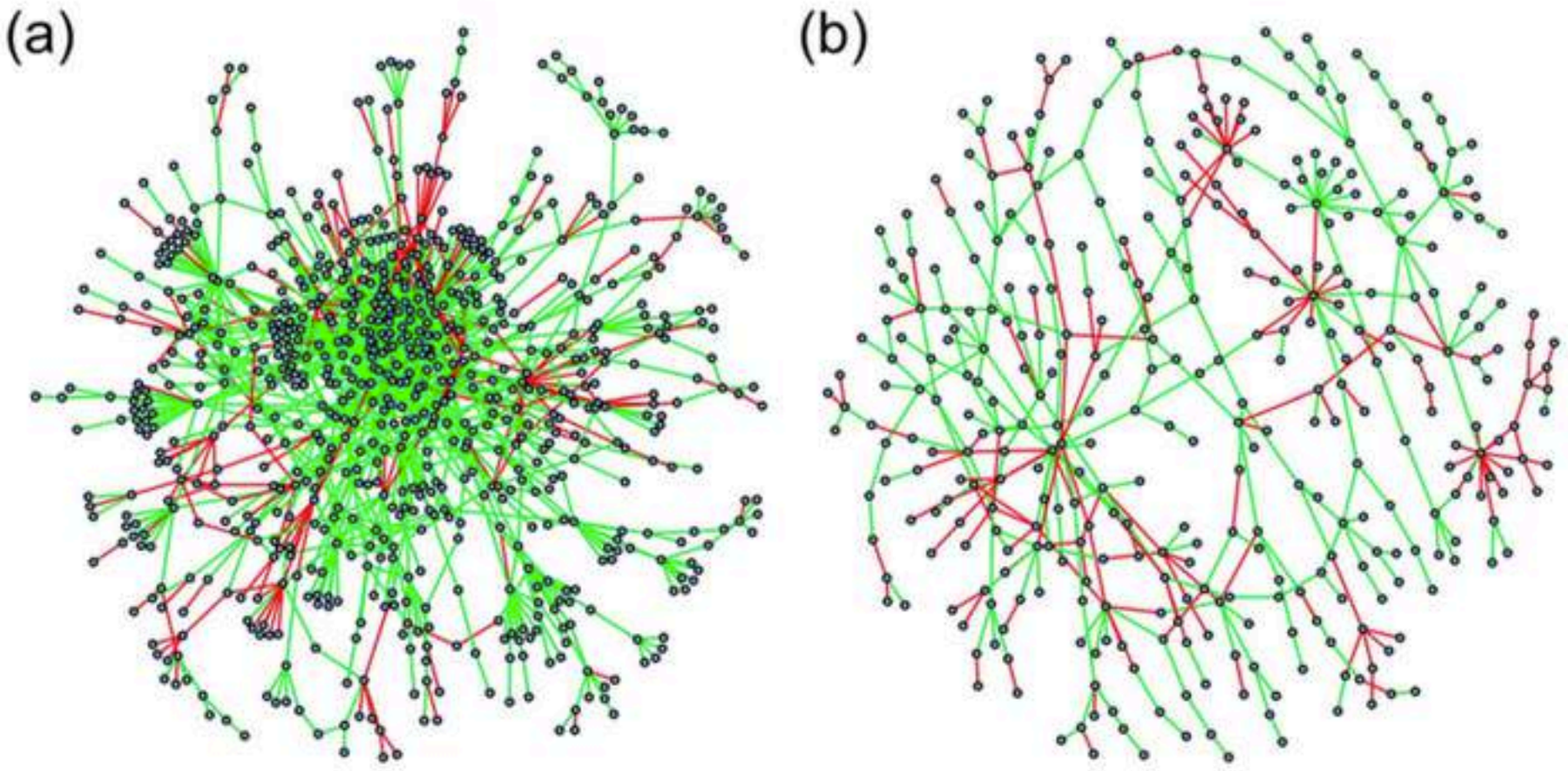

Figure 4. Larger significant subnetworks: network diagrams. Network edges displayed in green and red indicate positive and negative hazard ratios, respectively, for the DNAm network correlation measure corresponding to that interaction; these correspond, respectively, to an increase and decrease in 'network interaction co-ordinatedness' for worse disease prognosis. (a) the KIRC large subnetwork. (b) the LUAD large subnetwork. Further details about the corresponding network nodes (genes) for the top 5% of the degree distribution and top 25 significantly enriched gene sets appear in tables S5–6.

How to build a network if links are unknown?

OPEN ACCESS Freely available online

PLOS ONE

A DNA Methylation Network Interaction Measure, and Detection of Network Oncomarkers

Thomas E. Bartlett[1,3]*, Sofia C. Olhede[2,3], Alexey Zaikin[1]

January 2014 | Volume 9 | Issue 1 | e84573

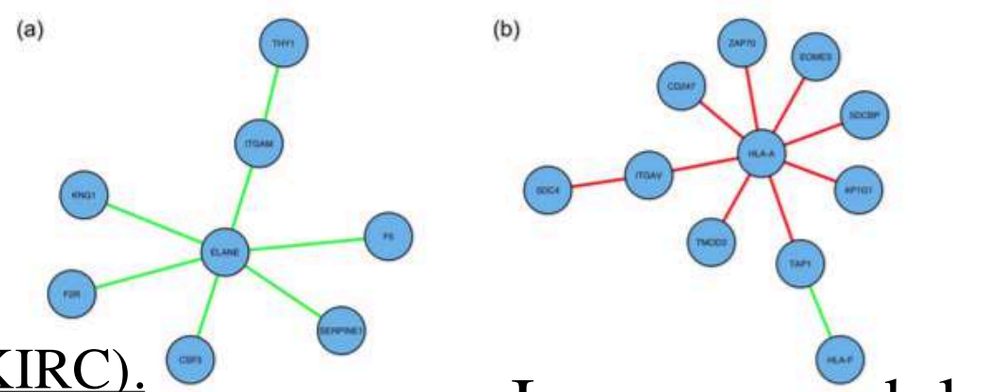

Wound healing module (KIRC).

Immune module

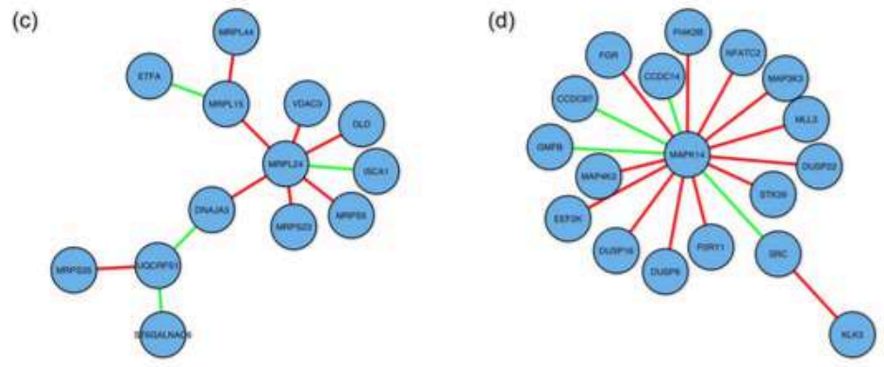

MAP-kinase module (LUSC).

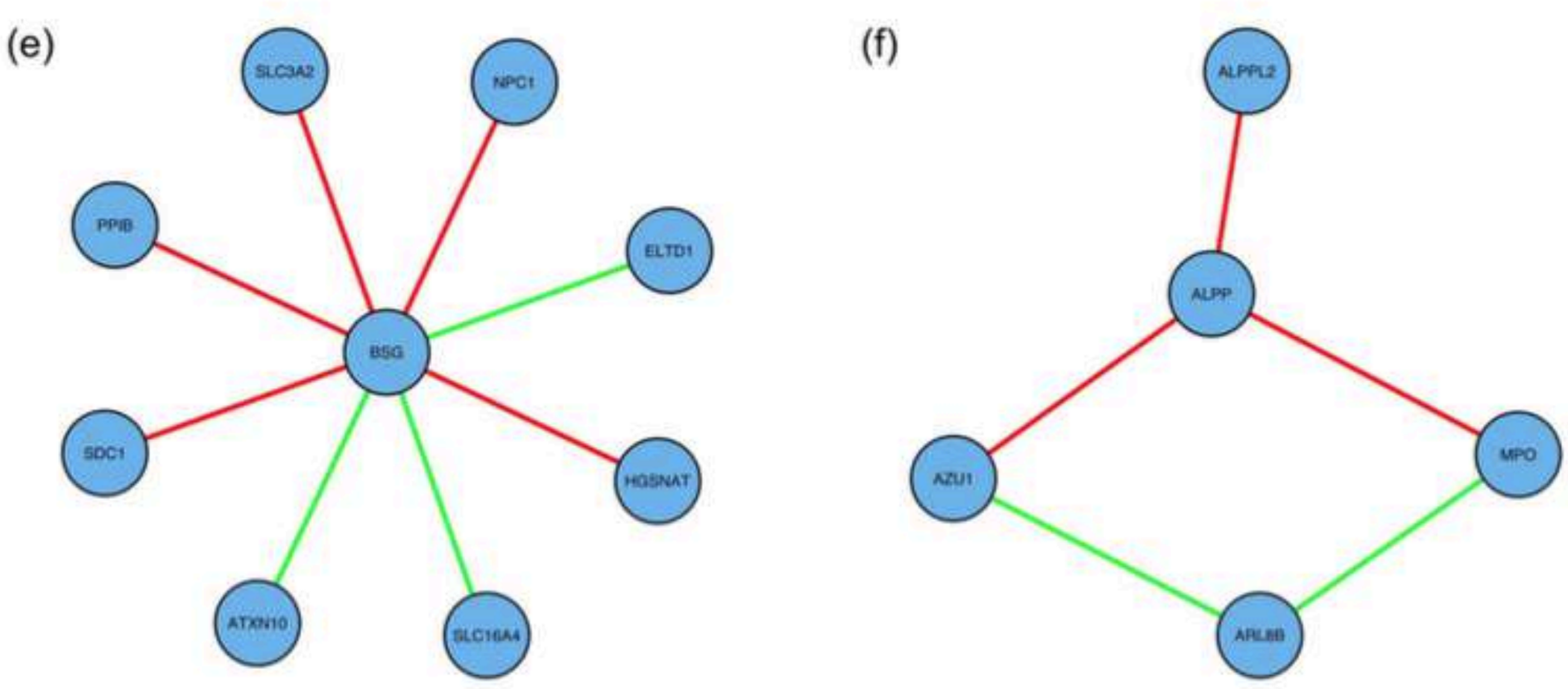

Figure 3. Smaller significant network modules: network diagrams. Network edges displayed in green and red indicate positive and negative hazard ratios, respectively, for the DNAm network correlation measure corresponding to that interaction; these correspond, respectively, to an

How to construct a network if links are unknown??

Bocaletti, Zanin 2014

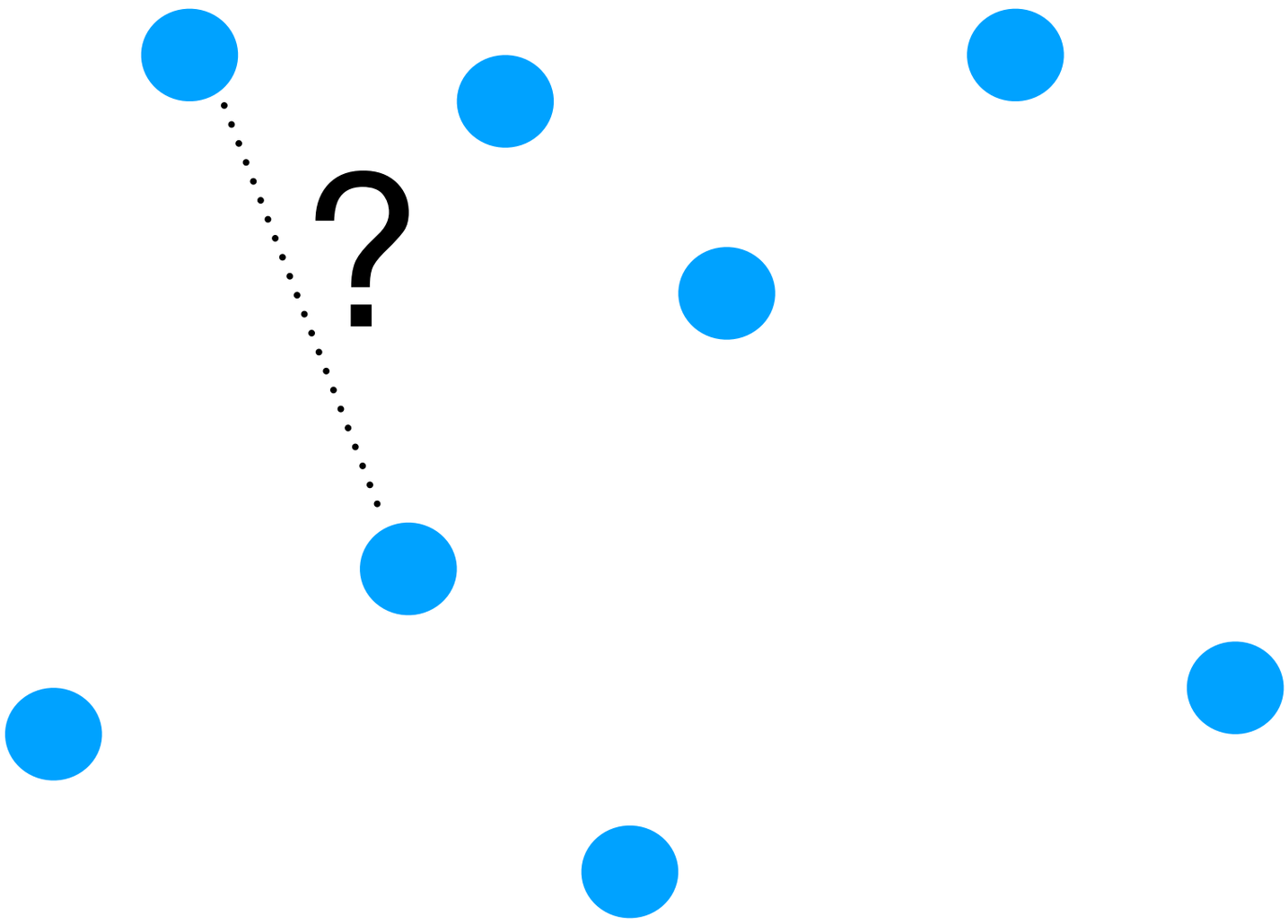

www.oncotarget.com Oncotarget, 2018, Vol. 9, (No. 32), pp: 22717-22726

Research Paper

Parenclitic networks for predicting ovarian cancer

Harry J. Whitwell[1], Oleg Blyuss[2], Usha Menon[3], John F. Timms[3] and Alexey Zaikin[3,4]

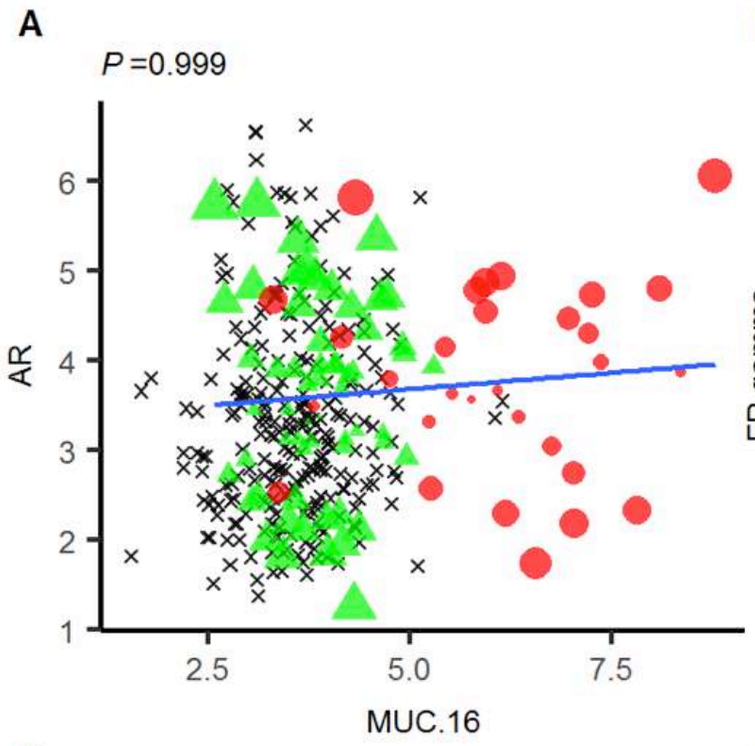

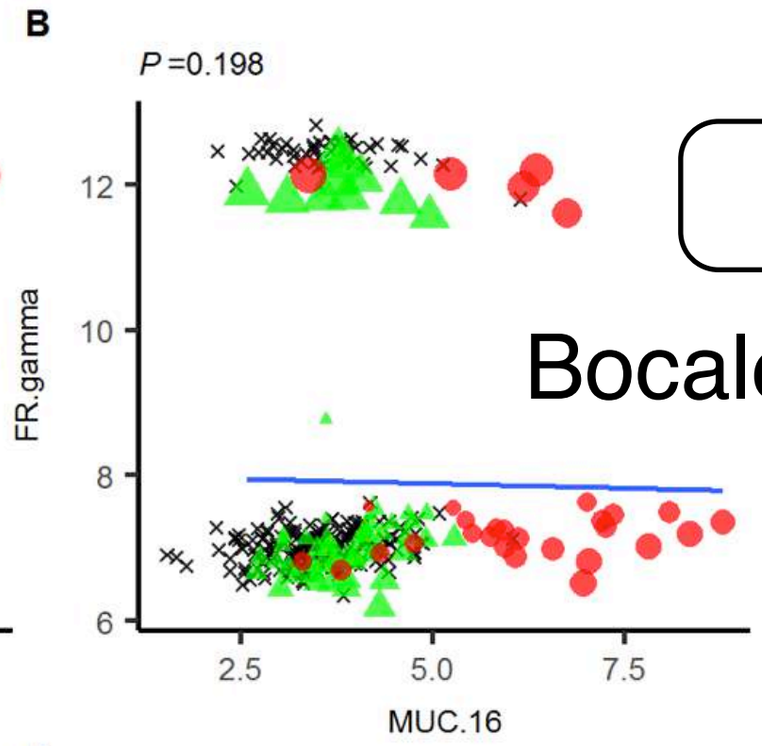

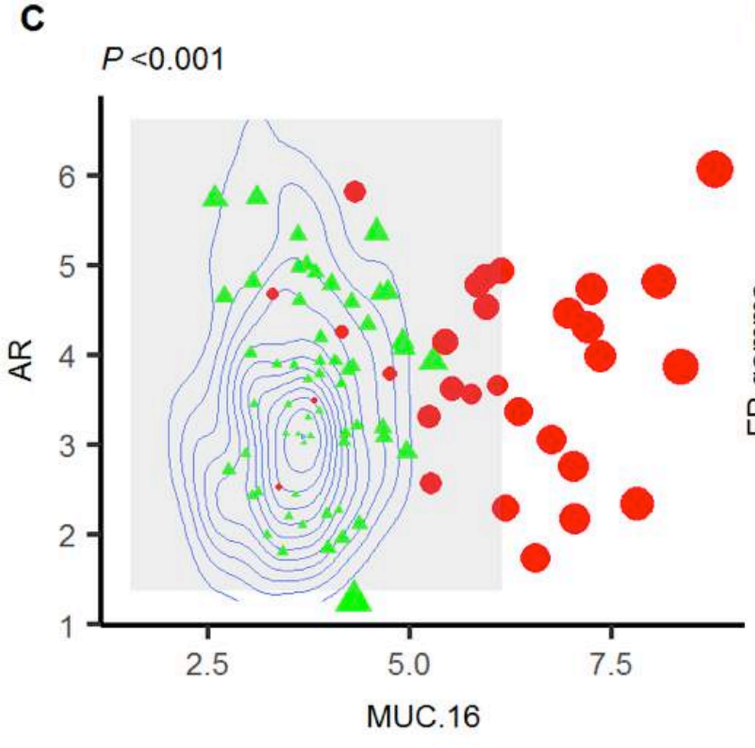

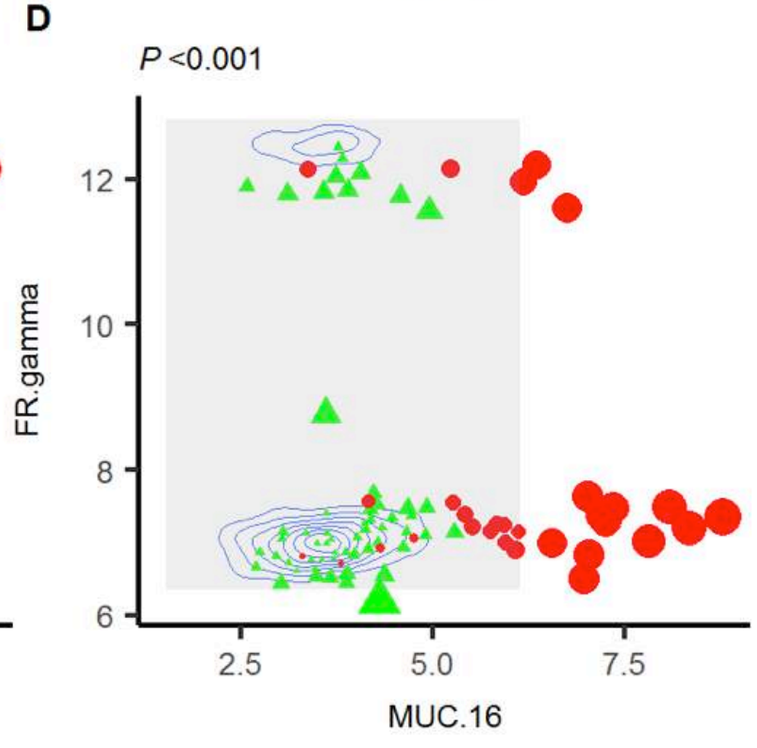

Network oncomarkers

Bocaletti, Zanin 2014

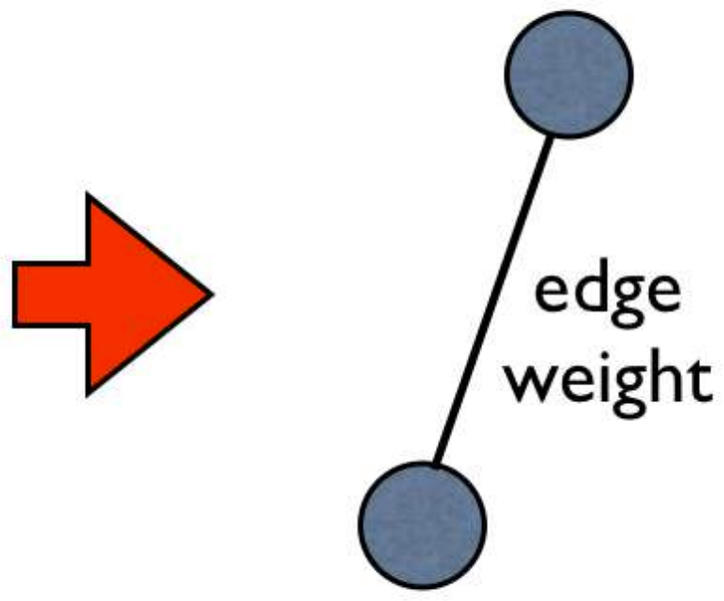

PLOS ONE

2017

RESEARCH ARTICLE

Parenclitic Network Analysis of Methylation Data for Cancer Identification

Alexander Karsakov[1], Thomas Bartlett[2], Artem Ryblov[1], Iosif Meyerov[3], Mikhail Ivanchenko[1], Alexey Zaikin[1,2]*

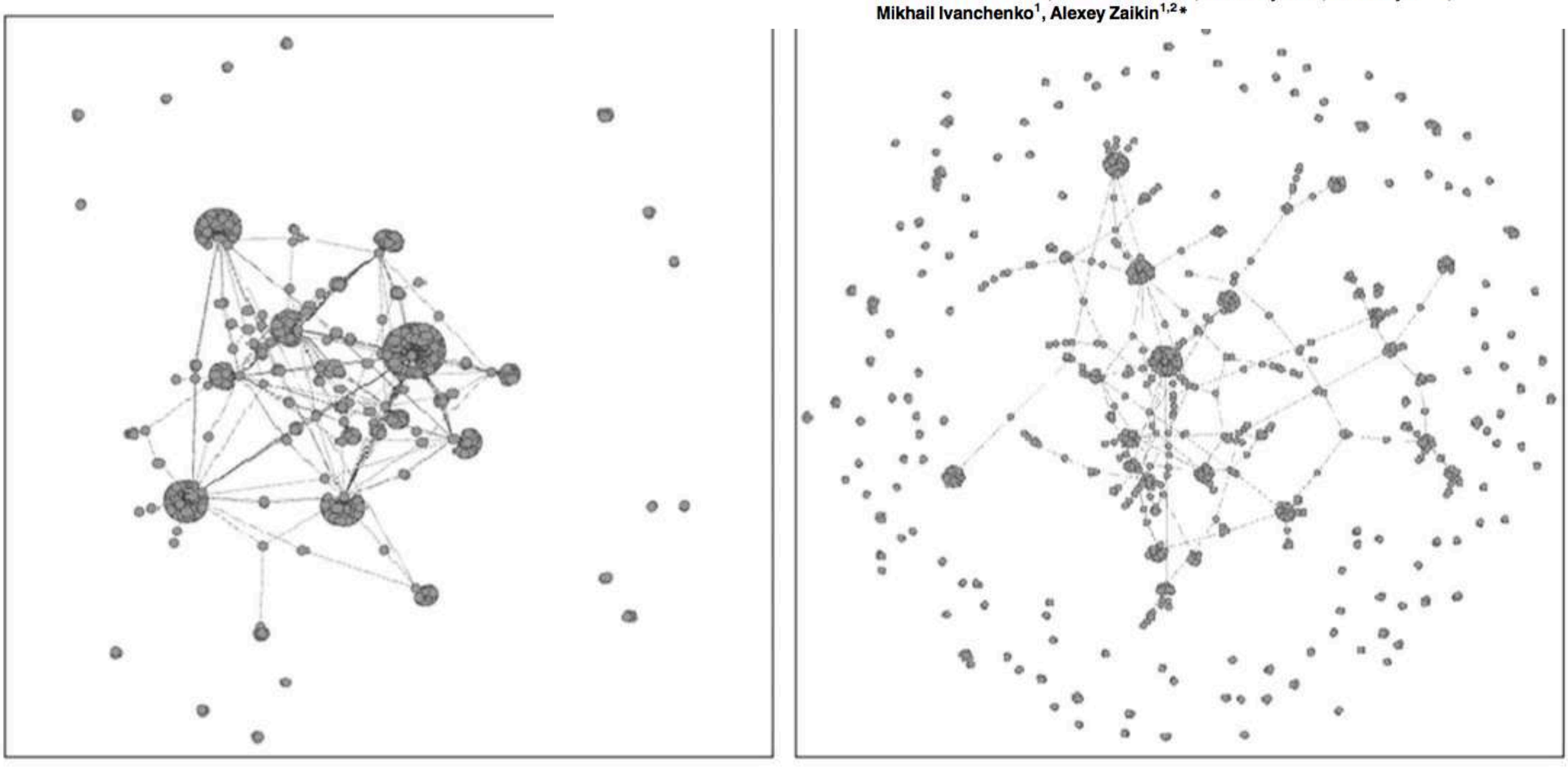

Fig 3. Typical examples of parenclictic networks constructed from gene methylation profiles for cancer (left) and normal (right) samples from BRCA data. Only a 1000 of the strongest edges and their incident nodes are shown. Note the pronounced modular structure for the cancer network.

www.oncotarget.com Oncotarget, 2018, Vol. 9, (No. 32), pp: 22717-22726

Research Paper

Parenclitic networks for predicting ovarian cancer

Harry J. Whitwell[1], Oleg Blyuss[2], Usha Menon[3], John F. Timms[3] and Alexey Zaikin[3,4]

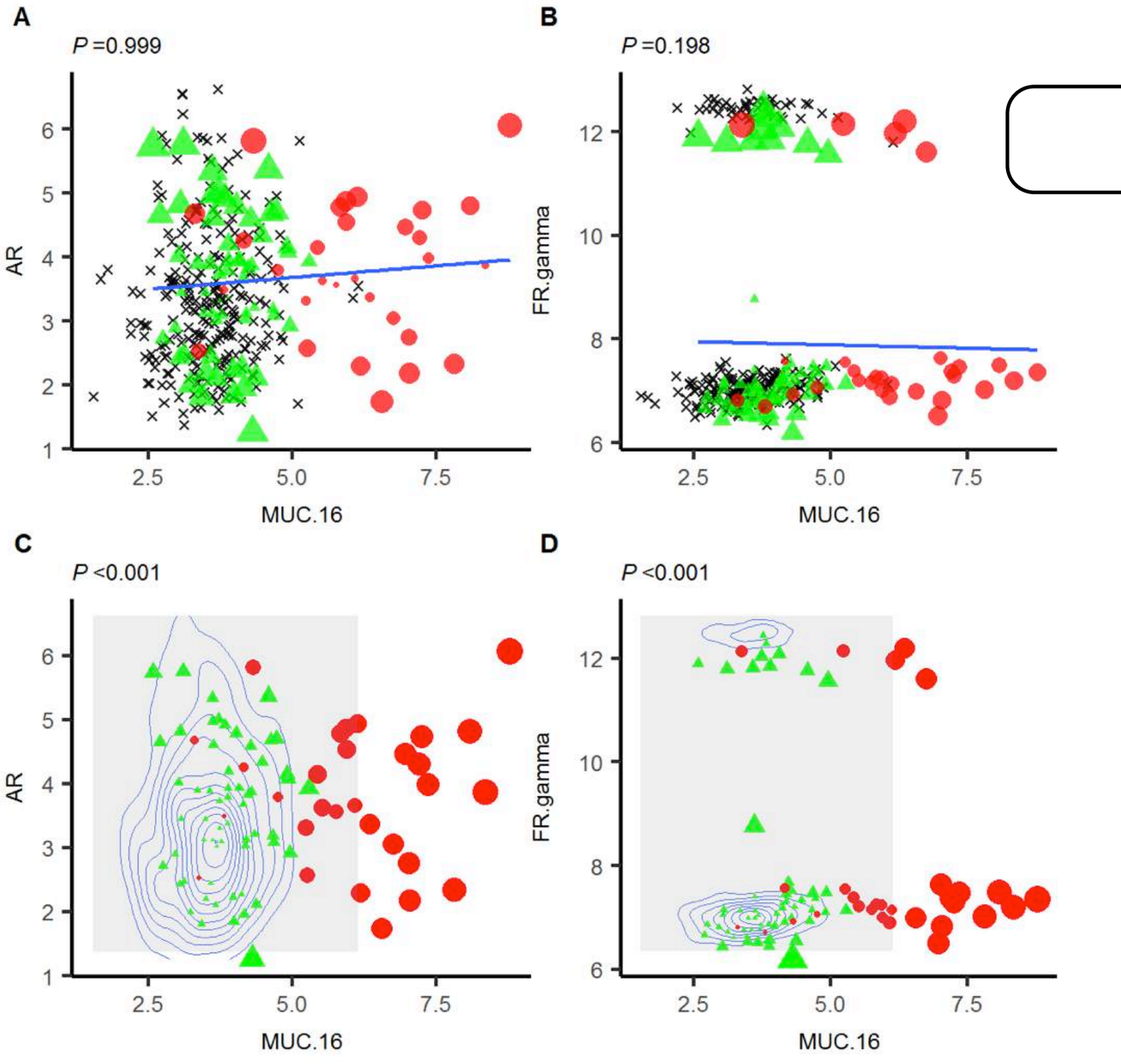

Network oncomarkers

edge weight

www.oncotarget.com Oncotarget, 2018, Vol. 9, (No. 32), pp: 22717-22726

Research Paper

Parenclitic networks for predicting ovarian cancer

Harry J. Whitwell[1], Oleg Blyuss[2], Usha Menon[3], John F. Timms[3] and Alexey Zaikin[3,4]

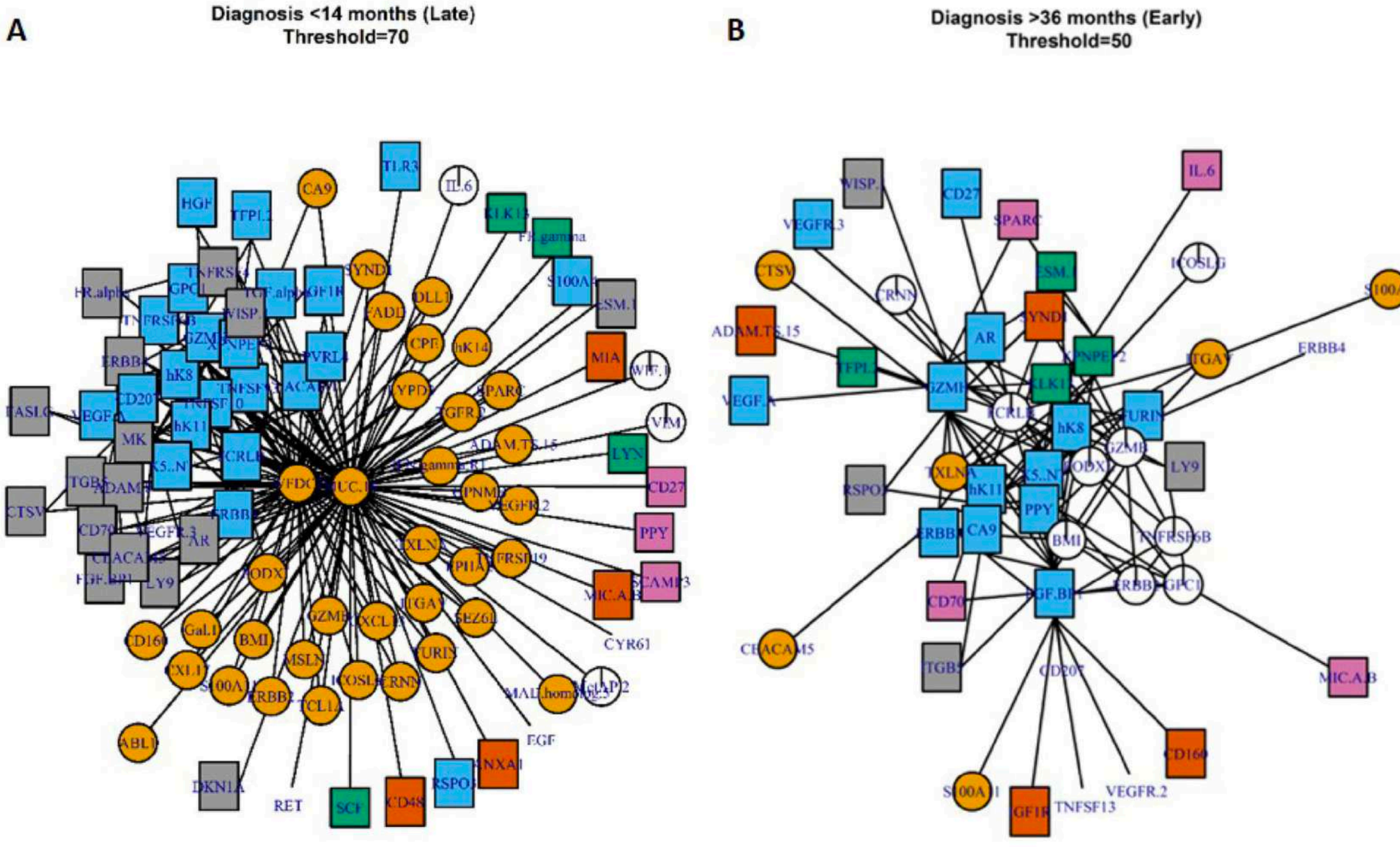

Synolitic networks
as applied to COVID-19 data

The patients admitted at the Charité University Hospital from early March to the end of June

7 Dec 2020

Coronavirus

Covid blood test can predict patient survival chances

Protein analysis provides digital picture of immune response and mortality risk, say scientists

Coronavirus - latest updates
See all our coronavirus coverage

Linda Geddes

Mon 7 Dec 2020 11.26 GMT

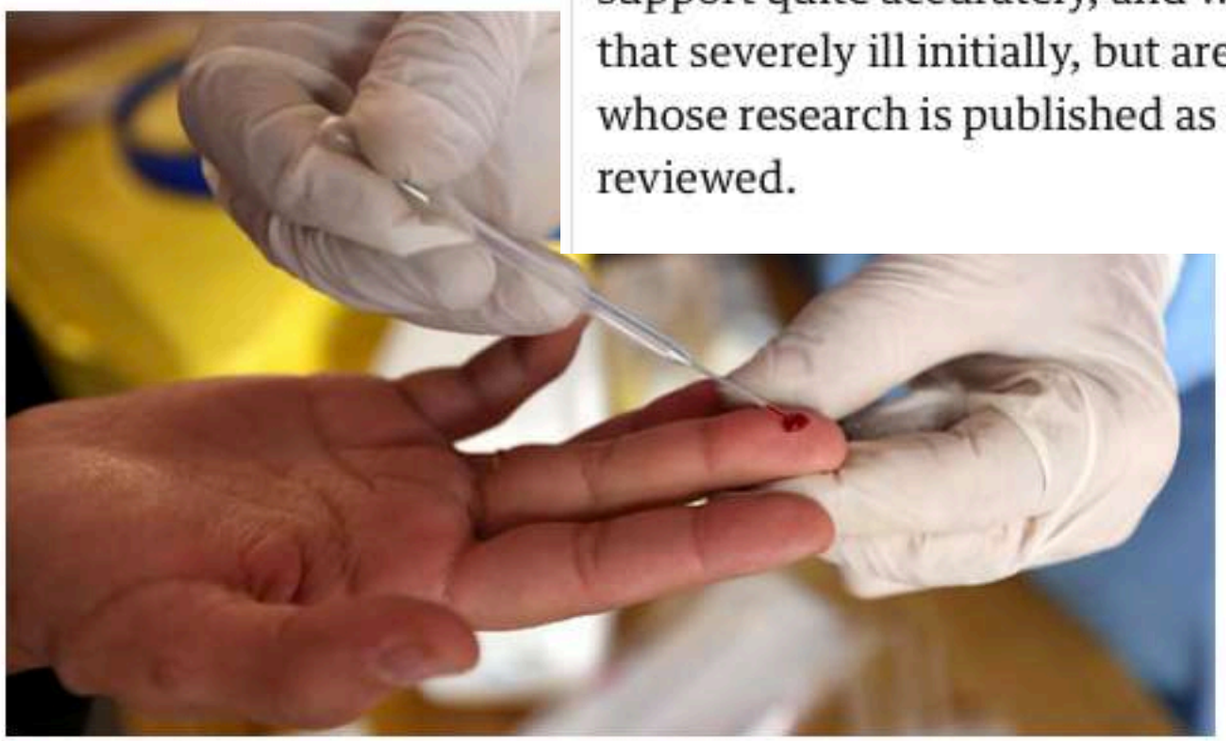

▲ It is unlikely that a blood test alone would ever be used to dictate which patients are allocated ICU beds. Photograph: Murtaja Lateef/EPA

A blood test has been developed that can predict whether Covid patients will need intensive care - or are even likely to survive - shortly after they develop symptoms.

"We can predict which patients will need oxygen support and ventilator support quite accurately, and we also have markers for patients who are not that severely ill initially, but are at high risk of getting worse," said Ralser, whose research is published as a preprint but has not yet been peer reviewed.

Cell Systems 2021
PLOS Digital Health 22

A huge-collaborative effort: 61 authors, 28 affiliations

Parenclitic Networks Predict Survival for Severely Ill Covid-19 Patients (Grade WHO = 7) Weeks Before Outcome with Extremely High Predictive Power

Tatiana Nazarenko

Harry J. Whitwell

Oleg Blyuss

John F. Timms

Alexey Zaikin

MRC Medical Research Council

a time-resolved deep clinical and molecular phenotyping of 139 adult patients with COVID-19 during hospitalization

Cell Systems

CellPress OPEN ACCESS

Cell Systems *12*, 1–15, July 21, 2021

Article

A time-resolved proteomic and prognostic map of COVID-19

Vadim Demichev,[1,2,3,27] Pinkus Tober-Lau,[4,27] Oliver Lemke,[1] Tatiana Nazarenko,[8,11] Charlotte Thibeault,[4] Harry Whitwell,[9,10,26] Annika Röhl,[1] Anja Freiwald,[1] Lukasz Szyrwiel,[2] Daniela Ludwig,[1] Clara Correia-Melo,[2]

+PLOS Digital Health 2022

Biomarkers that classify COVID-19 severity

based on clinical chemistry, enzyme activity, immunoprofile,
single cell sequencing, proteomics, and metabolomics.
High-throughput proteomic analysis - 180 samples/day.
309 proteins quantified in undepleted PLASMA using Scanning SWATH with short gradients.

D'Alessandro, A., Thomas, T., Dzieciatkowska, M., Hill, R.C., Francis, R.O., Hudson, K.E., Zimring, J.C., Hod, E.A., Spitalnik, S.L., and Hansen, K.C. (2020). ***Serum Proteomics in COVID-19 Patients: Altered Coagulation and Complement Status as a Function of IL-6 Level***. J. Proteome Res.

Laing, A.G., Lorenc, A., Del Molino Del Barrio, I., Das, A., Fish, M., Monin, L., Muñoz-Ruiz, M., McKenzie, D.R., Hayday, T.S., Francos-Quijorna, I., et al. (2020). ***A dynamic COVID-19 immune signature includes associations with poor prognosis***. Nat. Med. *26*, 1623–1635.

Liu, Y., Gao, W., Guo, W., Guo, Y., Shi, M., Dong, G., Ge, Q., Zhu, J., and Lu, J. (2020b). **Prominent coagulation disorder is closely related to inflammatory response and could be as a prognostic indicator for ICU patients with COVID-19**. J. Thromb. Thrombolysis.

Messner, C.B., Demichev, V., Wendisch, D., Michalick, L., White, M., Freiwald, A., Textoris-Taube, K., Vernardis, S.I., Egger, A.-S., Kreidl, M., et al. (2020). **Ultra-High-Throughput Clinical Proteomics Reveals Classifiers of COVID- 19 Infection.** Cell Syst *11*, 11-24.e4.

Overmyer, K.A., Shishkova, E., Miller, I.J., Balnis, J., Bernstein, M.N., Peters-Clarke, T.M., Meyer, J.G., Quan, Q., Muehlbauer, L.K., Trujillo, E.A., et al. (2020). **Large-scale Multi-omic Analysis of COVID-19 Severity**. medRxiv.

Schulte-Schrepping, J., Reusch, N., Paclik, D., Baßler, K., Schlickeiser, S., Zhang, B., Krämer, B., Krammer, T., Brumhard, S., Bonaguro, L., et al. (2020). **Severe COVID-19 Is Marked by a Dysregulated Myeloid Cell Compartment.** Cell *182*, 1419–1440.e23.

Shen, B., Yi, X., Sun, Y., Bi, X., Du, J., Zhang, C., Quan, S., Zhang, F., Sun, R., Qian, L., et al. (2020). **Proteomic and Metabolomic Characterization of COVID-19 Patient Sera.** Cell *182*, 59–72.e15.

Shu, T., Ning, W., Wu, D., Xu, J., Han, Q., Huang, M., Zou, X., Yang, Q., Yuan, Y., Bie, Y., et al. (2020). **Plasma Proteomics Identify Biomarkers and Pathogenesis of COVID-19.** Immunity.

Wynants, L., Van Calster, B., Collins, G.S., Riley, R.D., Heinze, G., Schuit, E., Bonten, M.M.J., Damen, J.A.A., Debray, T.P.A., De Vos, M., et al. (2020). **Prediction models for diagnosis and prognosis of covid-19 infection: systematic review and critical appraisal.** BMJ *369*, m1328.

Patient State	Score	Descriptor
Uninfected	0	No clinical or virological evidence of infection
Ambulatory	1	No limitation of activities
	2	Limitation of activities
Hospitalised - mild disease	3	No oxygen therapy
	4	Oxygen by mask or nasal prongs
Hospitalised - severe disease	5	Non-invasive ventilation or high-flow oxygen
	6	Intubation and mechanical ventilation
	7	Ventilation + additional organ support (vasopressors, RRT, ECMO)

WHO ordinal scale for clinical improvement in COVID-19 as used in the study (World Health Organisation 2020)

The patients admitted at the Charité University Hospital from early March to the end of June

All patients	No invasive mechanical ventilation			Invasive mechanical ventilation	
	Max WHO 3	Max WHO 4	Max WHO 5	Max WHO 6	Max WHO 7
139 100%	23 17%	32 23%	15 11%	6 4%	63 45%

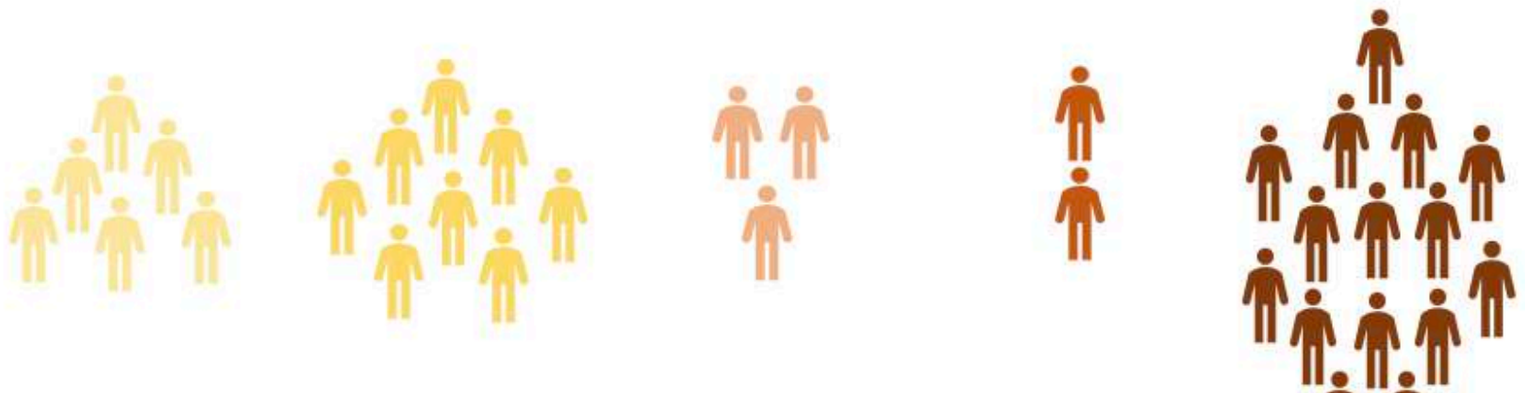

There were 139 patients, about half of whom were required invasive mechanical ventilation and half of whom are not. Among these people, 20 patients died, most of them (namely 17 people) are patients with a grade 7.

Charite cohort

139 patients from Charite hospital admitted with PCR confirmed CoVID. Serum and clinical diagnostics taken at multiple time points across course of stay – 687 plasma samples. 309 proteins quantified in undepleted PLASMA using Scanning SWATH with short gradients. Since mortality was predominantly associated with patients with a grade 7 (that is, the most severe patients), we selected only them. There were 63 people.

WHO grade 7 patients (63)

outcome (i.e. discharge or death) for them was not established

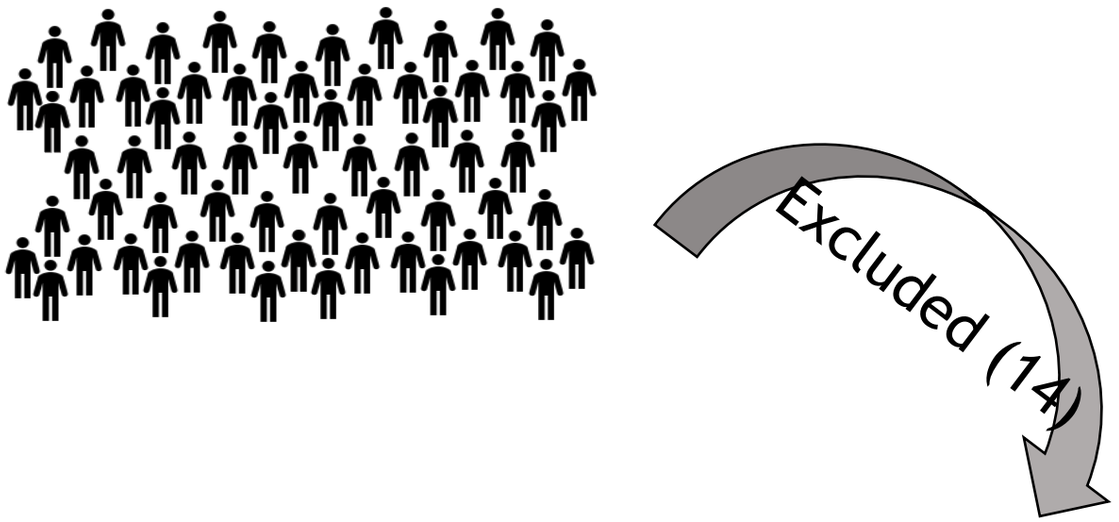

WHO grade 7 patients (63)

The remaining 49 patients were divided into a control group (or discharged patients) and a case group (or deceased patients).

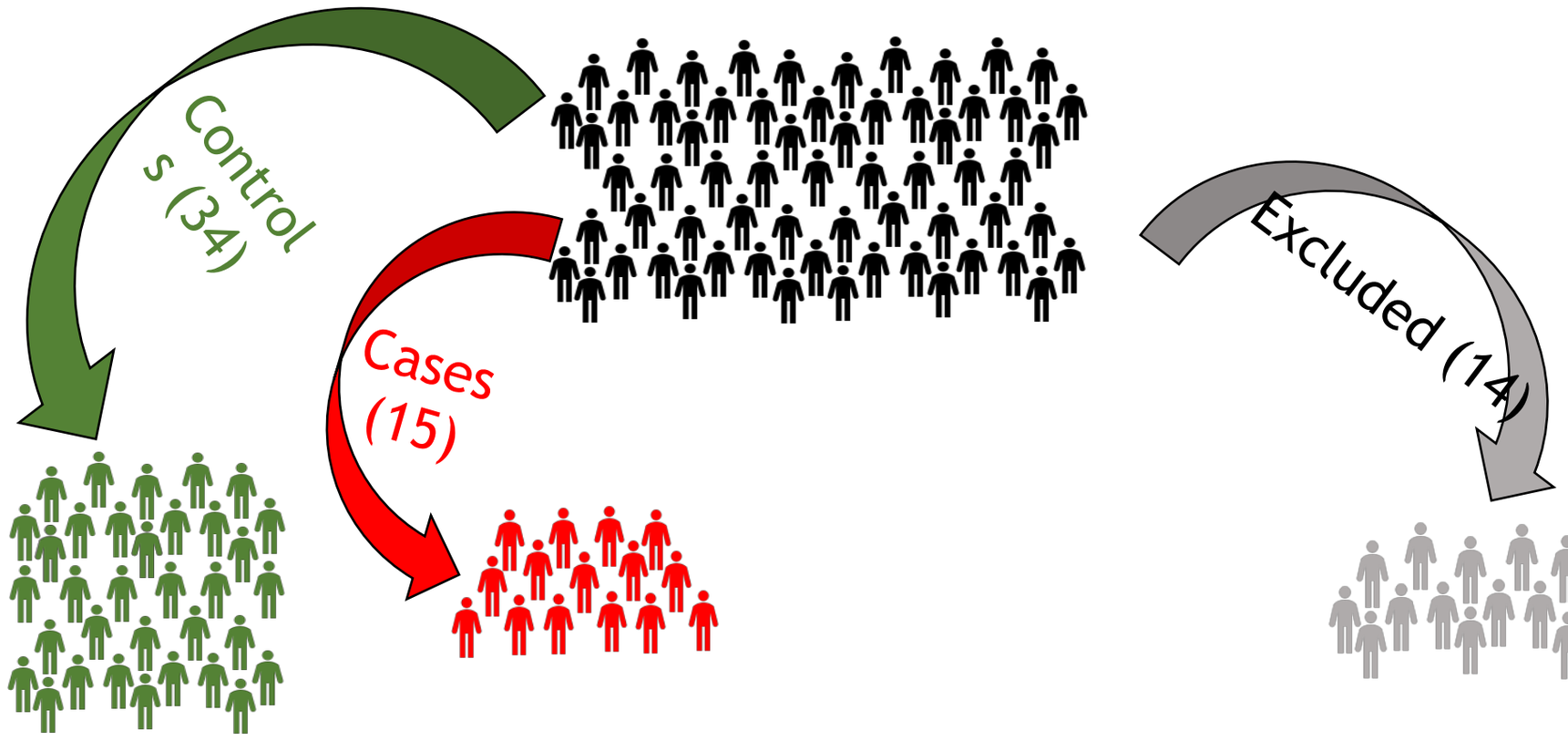

WHO grade 7 patients (63)

It should be especially noted that other machine learning algorithms did not give good quality on this dataset,
and only using of parenclitic networks approach allow us to obtain such a good results.

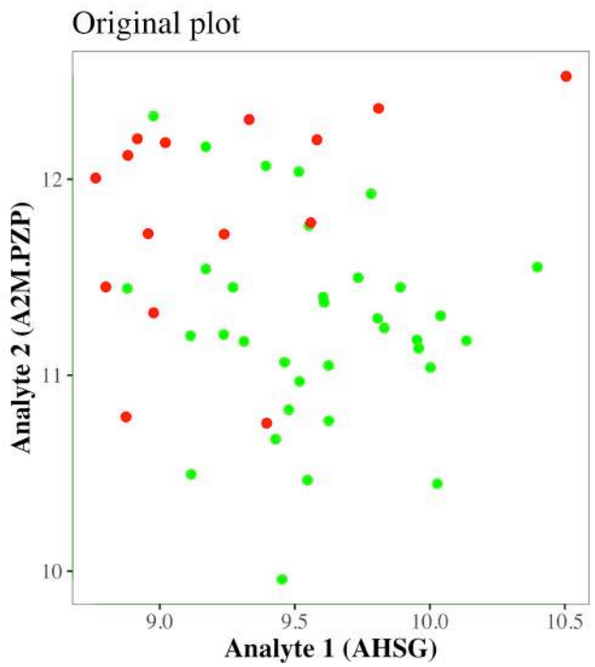

Synolitic Network Construction (SVM approach)

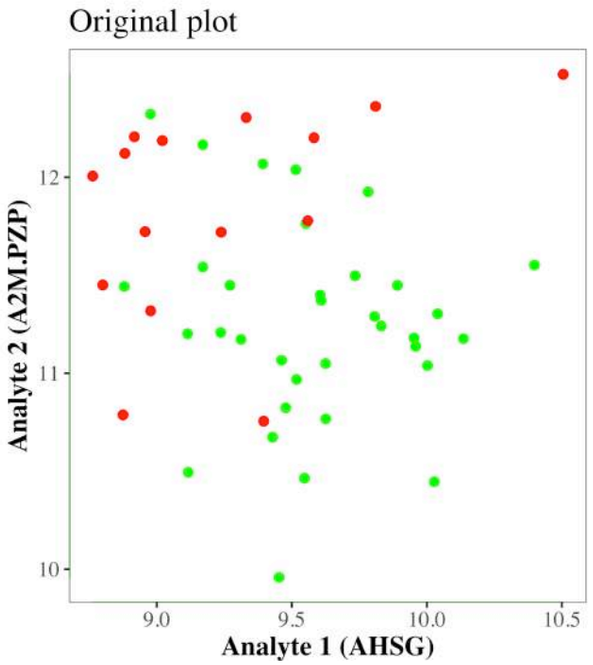

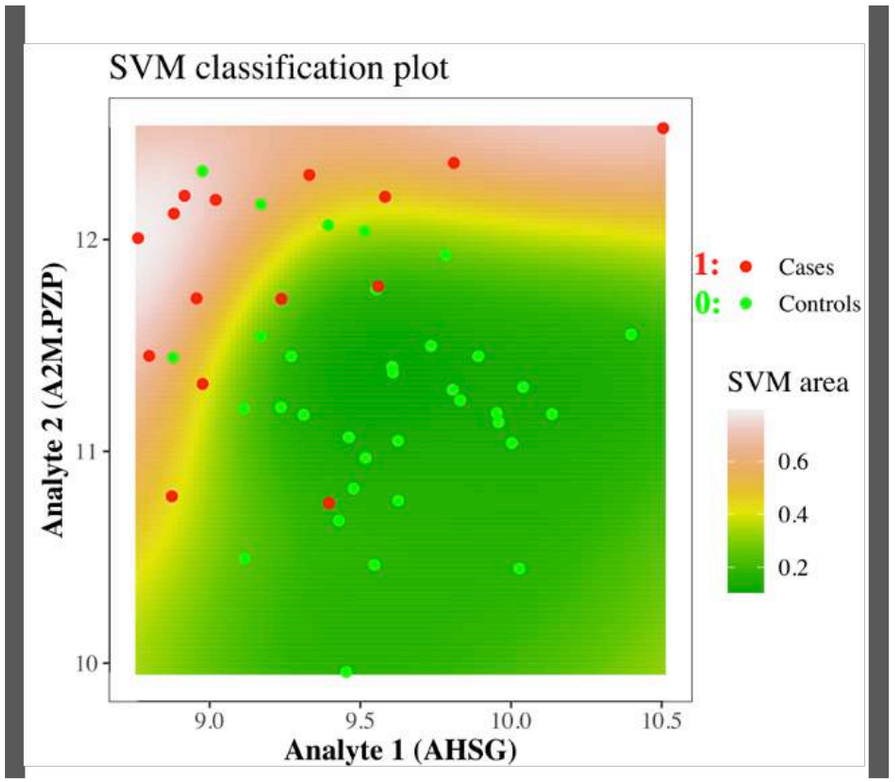

Synolitic Network Construction (SVM approach)

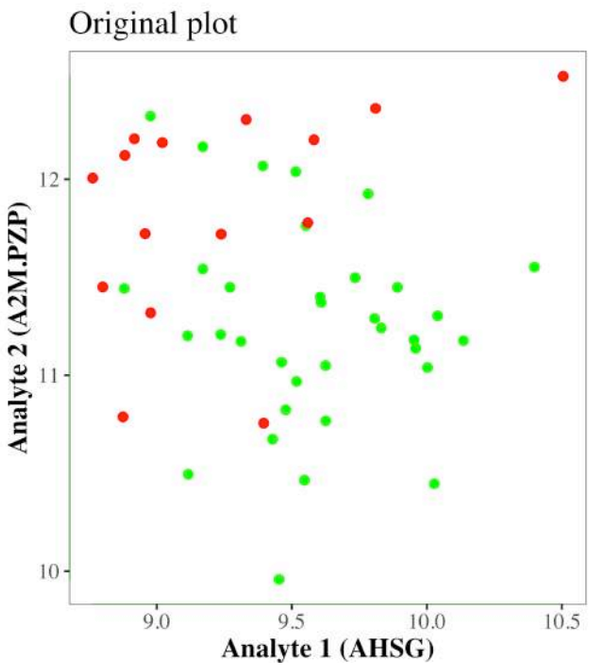

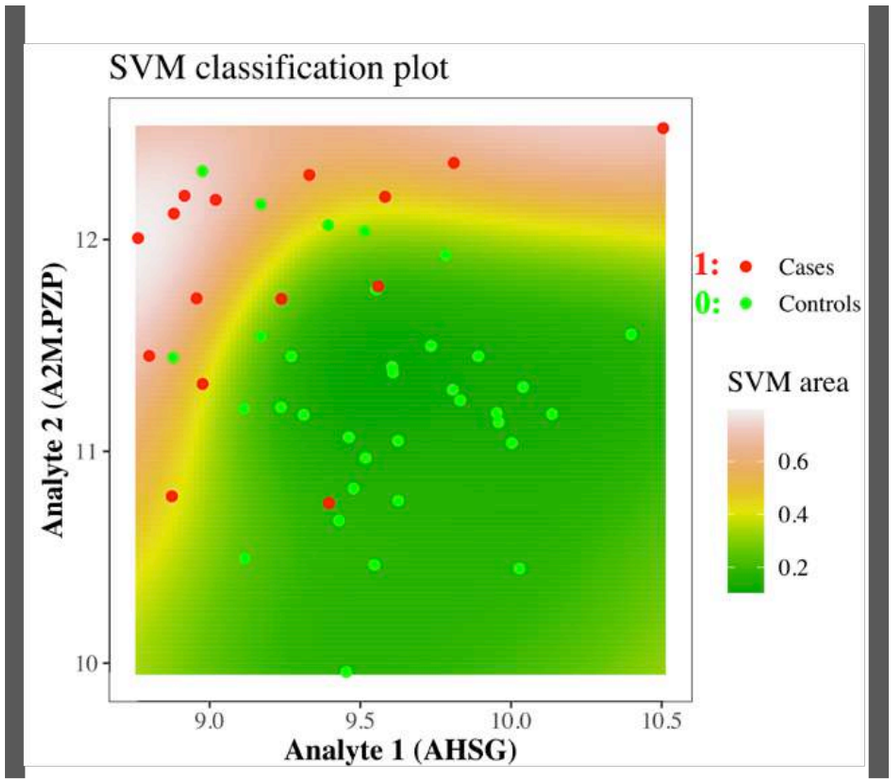

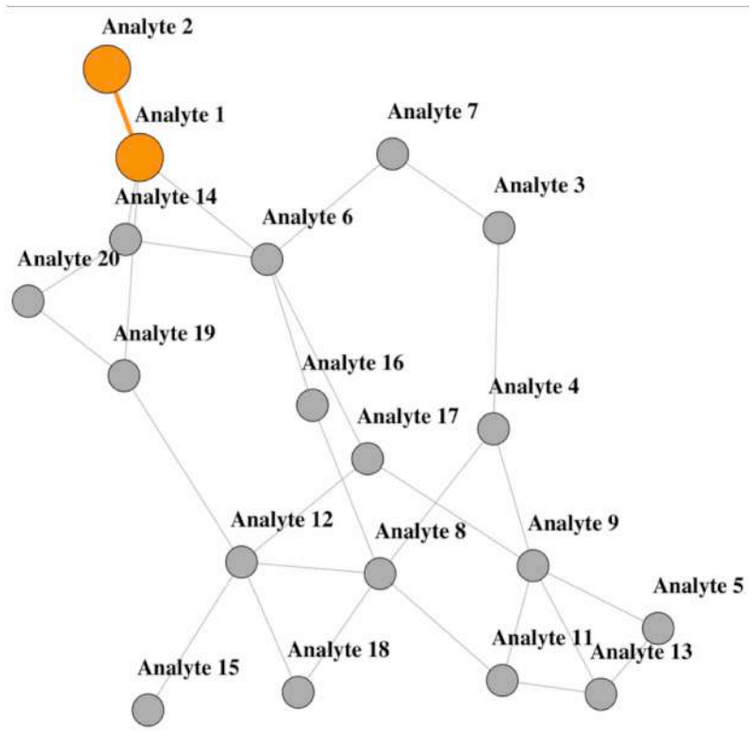

Synolitic Network Construction (SVM approach)

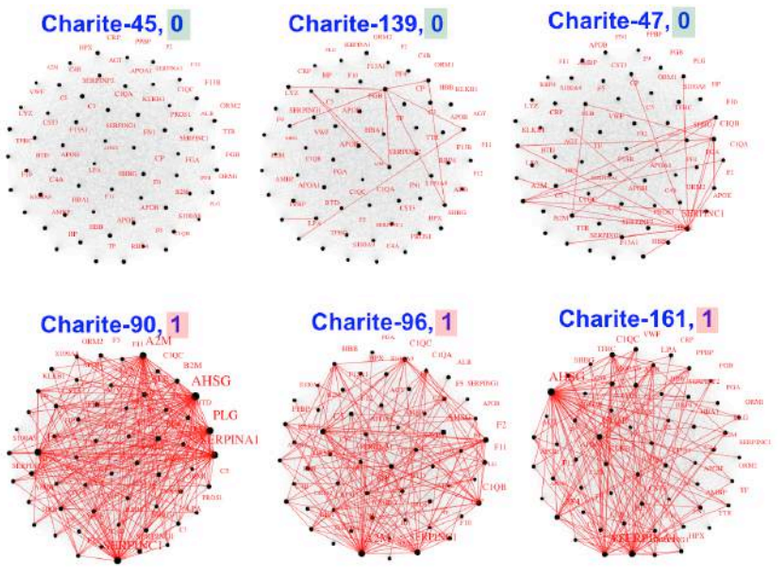

Calculate topological characteristics

Train a classifier

Binary classification problem on networks characteristics

Following cross-validation, the model showed excellent accuracy (AUC = 0.81) despite the median time from sampling to outcome being 39 days. You also can see interquartile range: from 16 to 64 days.
Especially amazing results (with AUC=1) we had on validation our model on completely independent dataset - 24 Covid-19 patients admitted to the Innsbruck Hospital in Austria.

COVID-19: survival prediction for critical (WHO grade 7) patients using parenclitic networks

Binary classification problem

For each sample construct a network, wherein nodes correspond to proteins

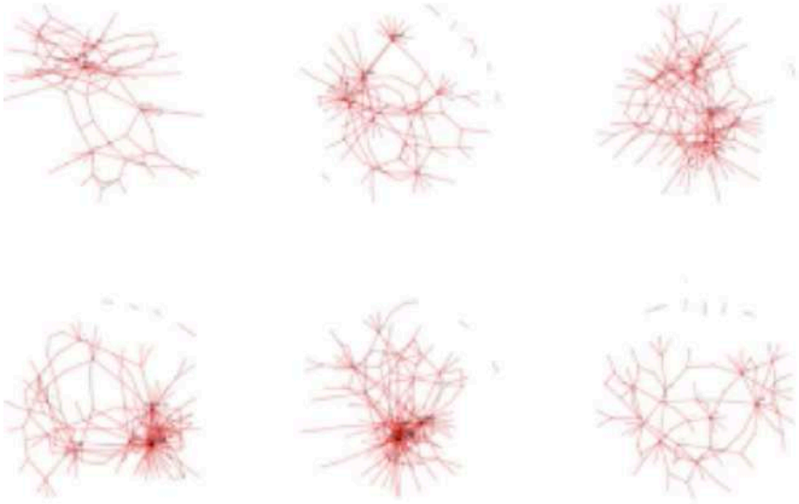

Calculate topological characteristics

Train a classifier

Ultra-fast proteomics: 180 samples / day

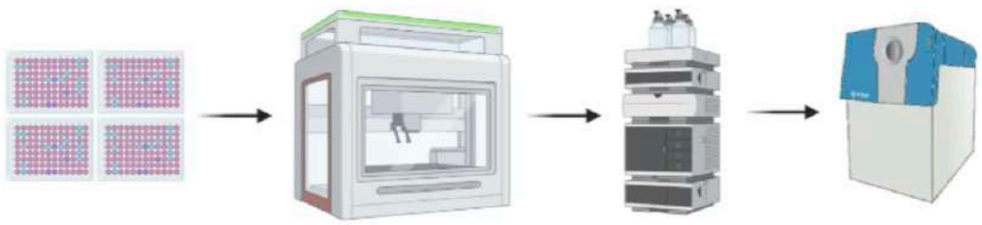

Sample preparation on four 96-well plates using a liquid-handling robot

High-flow (0.8 ml / min) 5-minute gradient 180 samples / day

SWATH-MS

Neural network-based software

Collaboration with
Tatiana Nazarenko
Harry Whitwell
Oleg Blyuss
Alexey Zaikin
John Timms

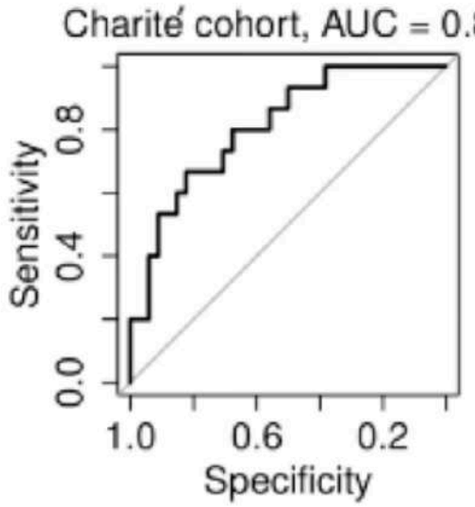

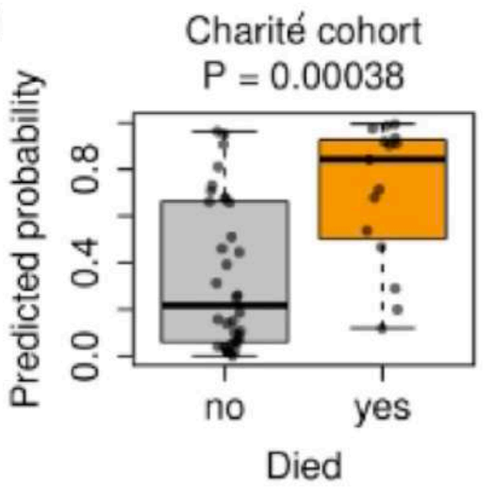

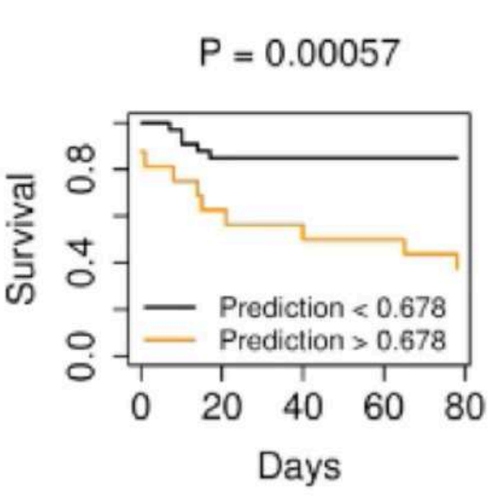

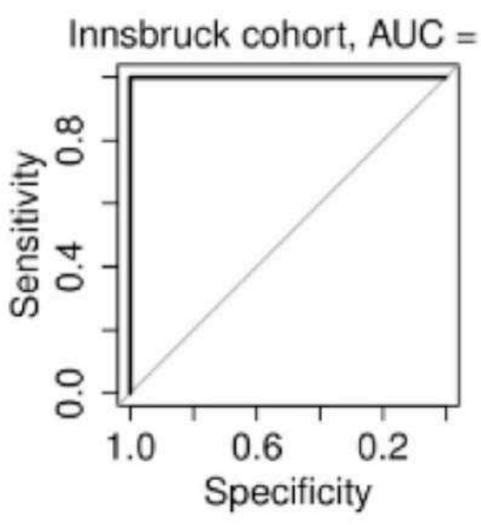

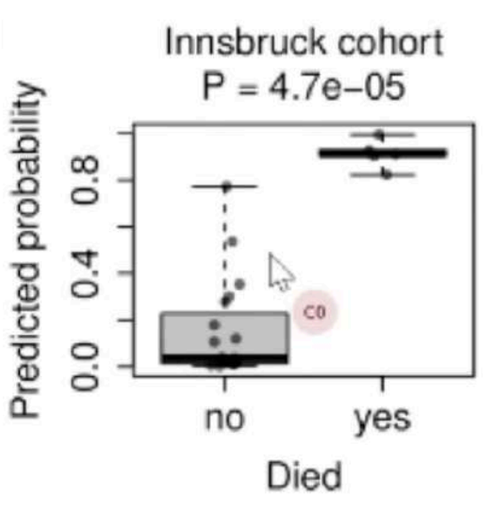

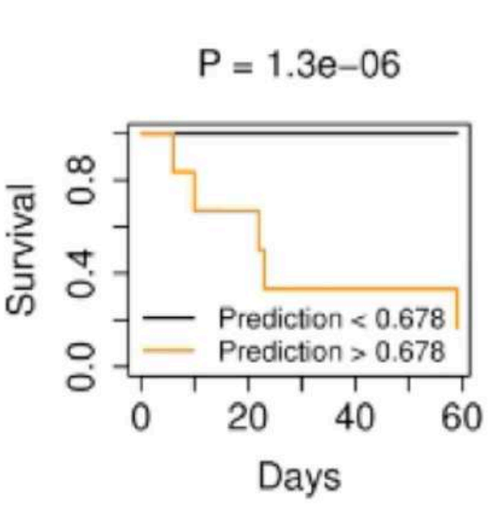

Age-related trajectories

Age-related trajectories of DNA methylation network markers: a parenclitic network approach to a family-based cohort of patients with Down Syndrome

M. Krivonosov[1], T. Nazarenko[2,*], M.G. Bacalini[3], M.V. Vedunova[1], C. Franceschi[1,3], A. Zaikin[1,2,4], and M. Ivanchenko[1]

Down Syndrome methylation data

As an application and demonstration of our implementation, we considered a publicly available dataset (GSE52588) in which whole blood DNA methylation was assessed by the Infinium HumanMethylation450 BeadChip in a cohort including persons affected by Down Syndrome (DS), their unaffected siblings (DSS) and their mothers (DSM)[20] (29 families in total).

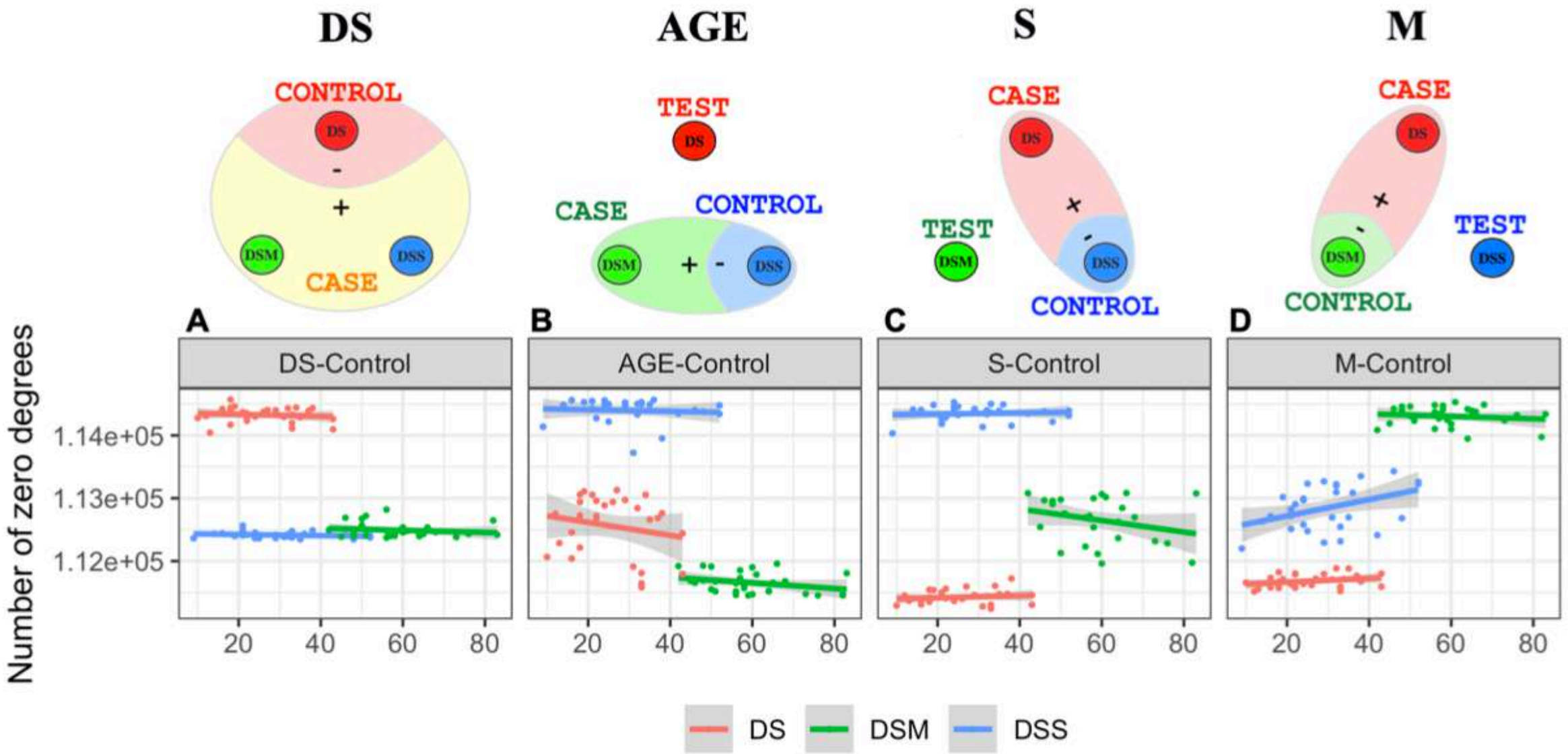

Figure 3. Top panel: Two sets of the data are used to find a boundary necessary to construct a network. This can be used to analyse the age-related trajectories for the third class (B-D). Bottom panel: examples how topological indices plotted vs age enable to find age related trajectories of network signatures. Dependence of characteristics (here, for example, only Number of zero degrees nodes) of individual networks in DS/AGE/S/M-network design versus AGE (A–D labels respectively). A) Down methylation network signature. B) Age-accelerated ageing in Downs. C) Hyper-ageing in DS. D) Divergence of trajectories in Downs and healthy sibs. Plots for all other characteristics can be found in Supporting Information.

But how age accelerated ageing in Downs will depend on a biological age estimated with well- established Horvath's clock? This is shown in the Fig. 4. We found a very surprising behaviour when we plotted topological indices versus residuals, i.e., a difference between a passport age and biological age. DS are closer to mothers, and develop with age towards mothers, i.e., their network features are more similar to mothers, the more is age acceleration. However, we find that even for DS with decelerated ageing, their methylation network signature has a trend towards older mothers. Probably, this can be explained by the fact that Horvath's methylation clock has been developed for healthy people and it does not work so well for DSS. In contrast to it, our approach always shows age acceleration in patients with DS.

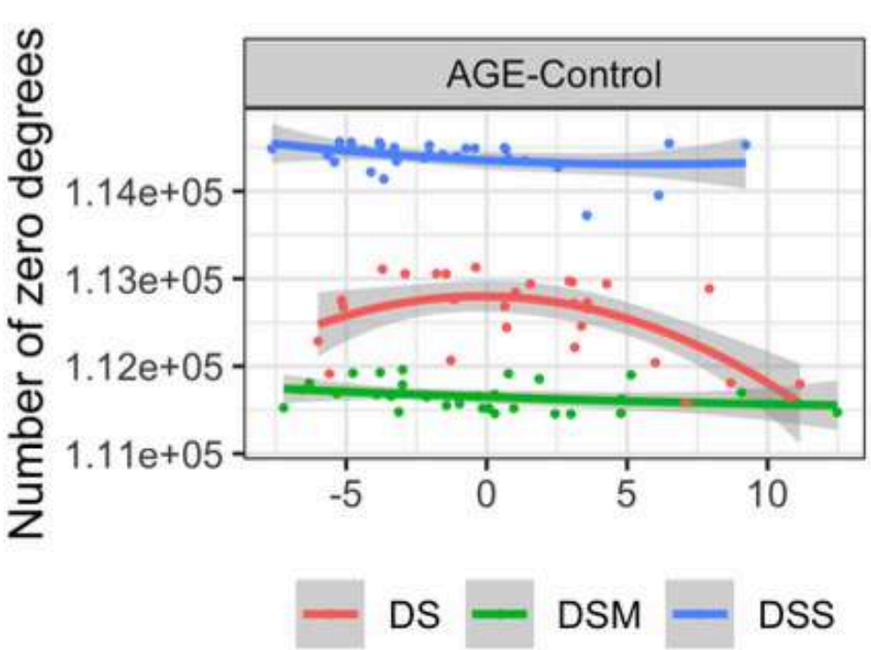

Figure 4. Dependence of characteristics (here, for example, only Number of zero degrees nodes) of individual networks in RESIDUALS, i.e., a difference between passport and biological age. Above zero along x-axis we have accelearted ageing, below - deccelerated. Still, in both cases, DS methylation network signature is closer to mothers. Plots for all characteristics can be found in Supporting Information.

How good are Synolitic Network Classification

Impact Factor 4.599 | CiteScore 3.7
More on impact ›

frontiers in Genetics | Statistical Genetics and Methodology

THIS ARTICLE IS PART OF THE RESEARCH TOPIC
Prediction and Explanation in Biomedicine using Network-Based Approaches
View all 10 Articles ›

ORIGINAL RESEARCH article

Front. Genet., 20 October 2021 | https://doi.org/10.3389/fgene.2021.733783

Parenclitic and Synolytic Networks Revisited

Tatiana Nazarenko[1]*, Harry J. Whitwell[2,3,4,5], Oleg Blyuss[1,4,6,7] and Alexey Zaikin[1,4,5]

- Sphere-models: Controls: points with R < 0.5, Cases: points with 0.5<R <1)
- Types of Spheres:

- **Ideal Spheres Model** – all parameters are sphere parameters
- **Noisy Spheres Model** – 50 noise parameters were added for sphere parameters
- **Broken Spheres Model** – half sphere parameters were changed by noise parameters

Synthetic Data (SPHERES)

- For all modelling, we considered all possible combinations of
- *Sphere Dimensions*: (2, 3, 10, 30, 60, 90, 120, 150);
- number of *Case TRAIN samples*: (15, 65, 115, 165, 215, 265)
- number of *Controls TRAIN samples*: (15, 65, 115, 165, 215, 265).

- Numbers of *Case TEST samples* and *Controls TEST samples* were calculated as 25% of corresponding *TRAIN* numbers.

Examples of connections creating by different types of PN approaches

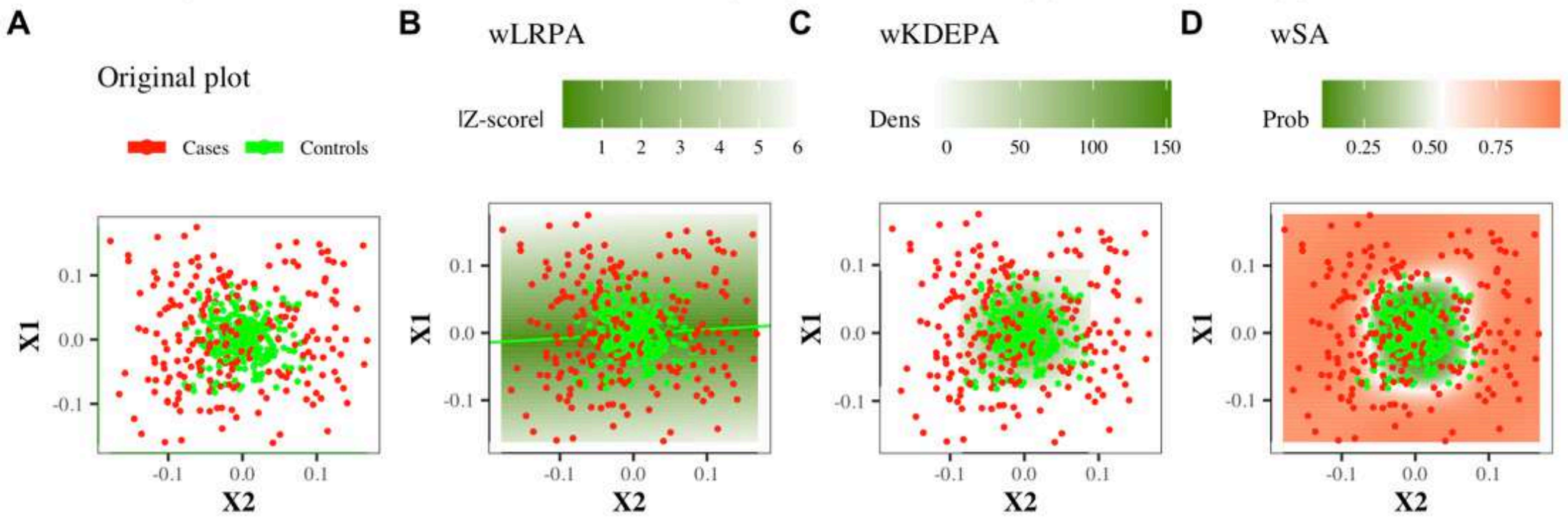

Main advantages:

Visualisation

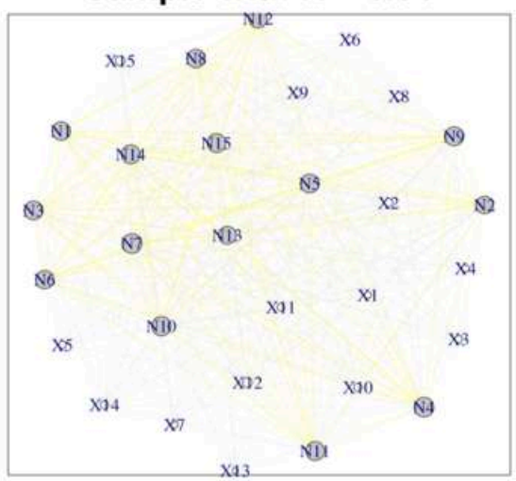

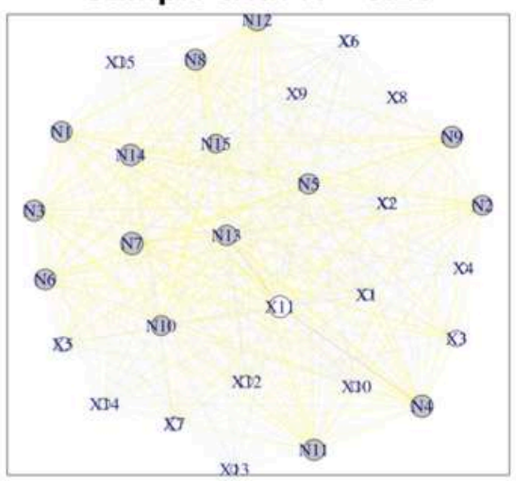

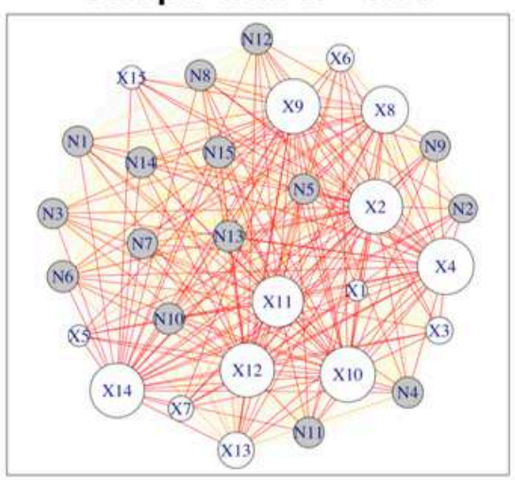

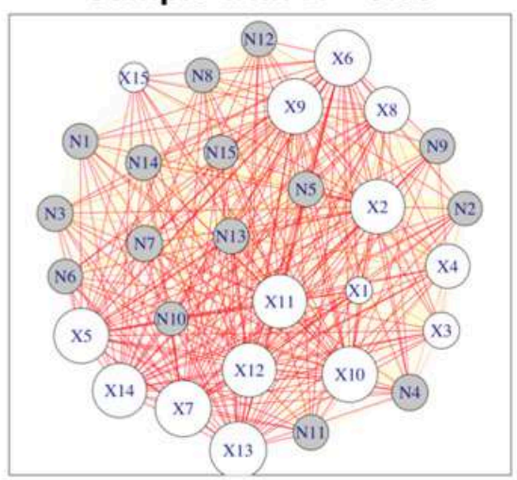

Main advantages:

Parenclitic approaches on average demonstrate superiority to other ML methods in situations where sample size is small relative to the number of features

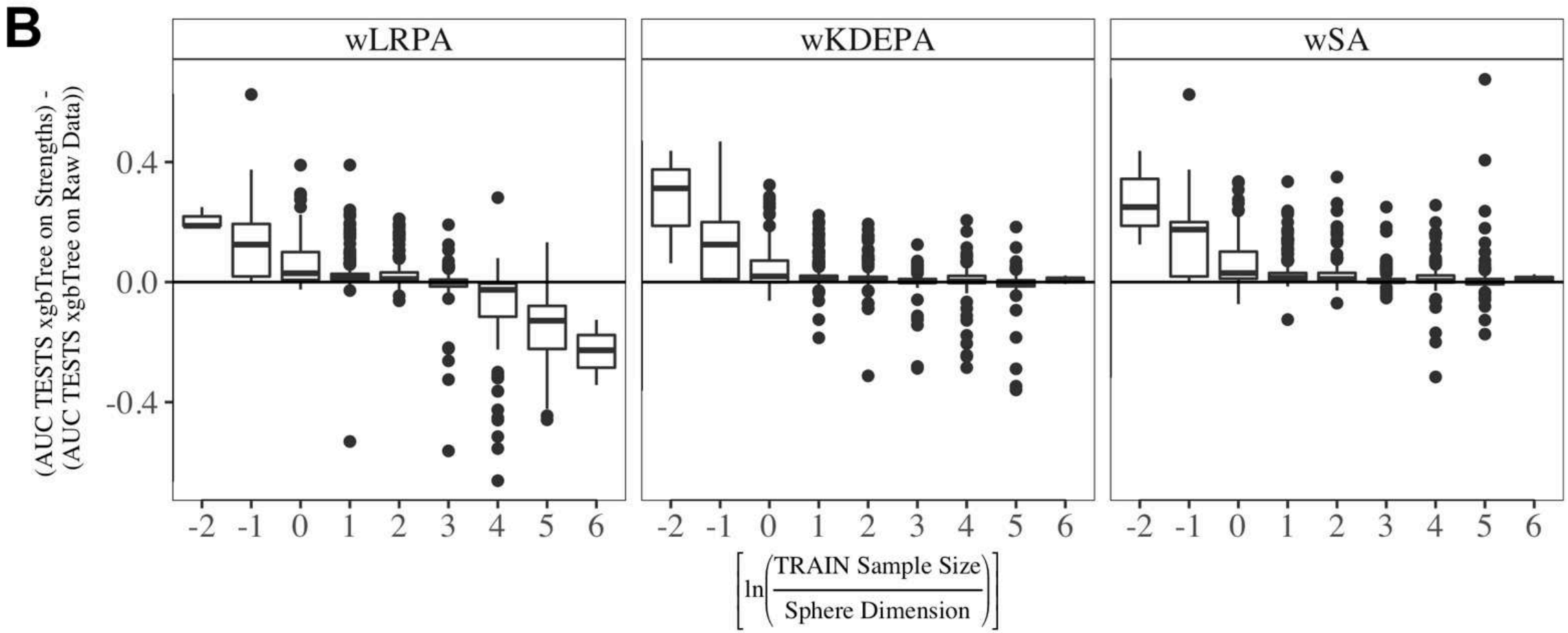

REAL DATA
https://archive.ics.uci.edu

N	Dataset	Number of Features	Samples	Cases	Controls	Area
1	Banknote (Ban, 2013)	4	1372	610	762	Computer
2	Blood (Blo, 2008)	4	748	178	570	Business
3	Vertebral-2c (Ver, 2011)	6	310	210	100	**Medicine**
4	Breast cancer (Bre, 1995)	10	699	241	458	**Medicine**
5	ILPD (ILP, 2012)	10	583	167	416	**Medicine**
6	PLRX (PLR, 2012)	12	182	52	130	Computer
7	Climate (Cli, 2013)	18	540	494	46	Physical
8	Diabetic (Dia, 2014)	19	1151	611	540	**Medicine**
9	SPECT (SPE, 2001)	22	267	212	55	**Medicine**
10	Ionosphere (Ion, 1989)	33	351	126	225	Physical
11	QSAR (QSA, 2013)	41	1055	356	699	Chemical
12	SPECTF (SPE, 2001)	44	267	212	55	**Medicine**
13	SONAR (SON, N/A)	60	208	97	111	Physical
14	Cortex (Cor, 2015)	77	1080	510	570	**Medicine**
15	URBAN (URB, 2014)	147	675	122	553	Physical
16	Arrhythmia (Arr, 1998)	260	452	245	207	**Medicine**

Parenclitic Synolitic

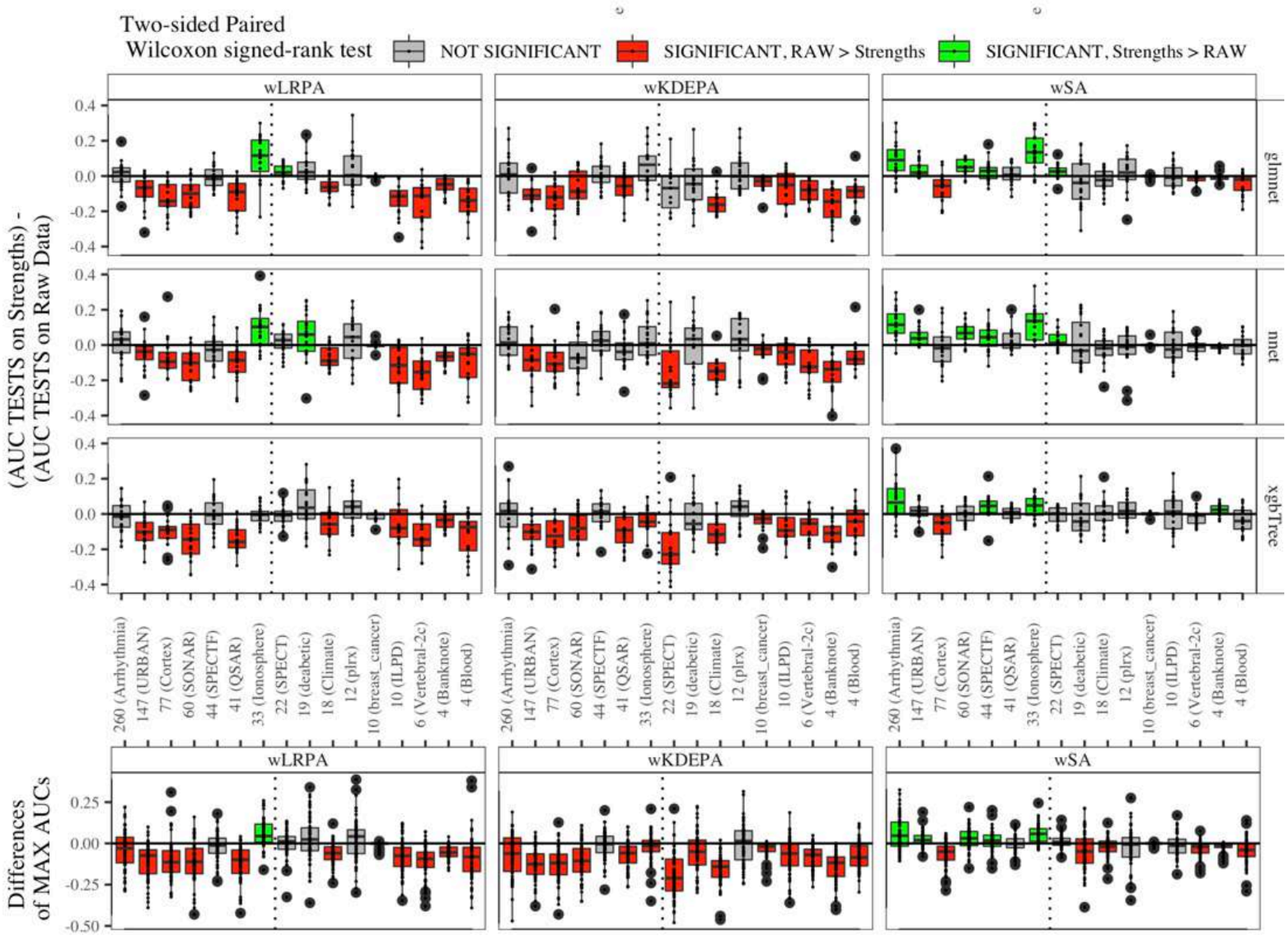

Open questions and ongoing work:

1. Comparison with Correlation graphs

2. Longitudinal Synolitic Networks

3. Graph-based Neural Networks

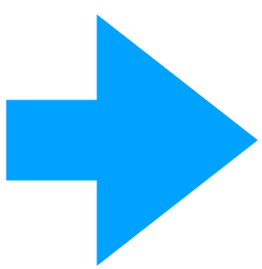

Personal Patient Tool?

- Key papers:
- finding longitudinal oncomarkers- License obtained!

Published OnlineFirst July 3, 2018; DOI: 10.1158/1078-0432.CCR-18-0208

Precision Medicine and Imaging

Clinical Cancer Research

Comparison of Longitudinal CA125 Algorithms as a First-Line Screen for Ovarian Cancer in the General Population

Oleg Blyuss[1], Matthew Burnell[1], Andy Ryan[1], Aleksandra Gentry-Maharaj[1], Inés P. Mariño[1,2], Jatinderpal Kalsi[1], Ranjit Manchanda[1,3], John F. Timms[1], Mahesh Parmar[4], Steven J. Skates[5], Ian Jacobs[1,6,7], Alexey Zaikin[1,8], and Usha Menon[1]

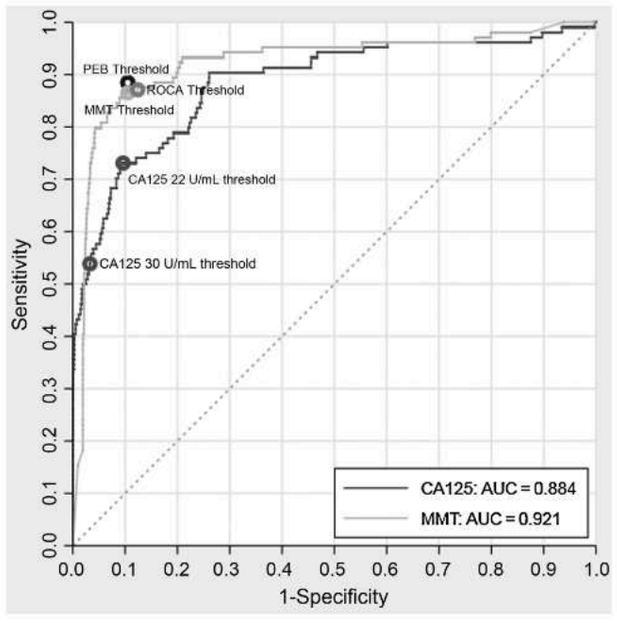

Figure 1.
Performance characteristics of CA125 interpreted using MMT, threshold rules, PEB and ROCA for detection of iEOC/PPC cases. Circle points give particular values of sensitivity and specificity provided by MMT and PEB corresponding to cutoff values obtained from the training set (MMT and PEB), CA125 using 22 and 30 U/mL cutoff values and ROCA as reported in ref. (6). Abbreviations: PEB, parametric empirical Bayes; MMT, method of mean trends; CA125, cancer antigen 125; AUC, area under roc-curve.

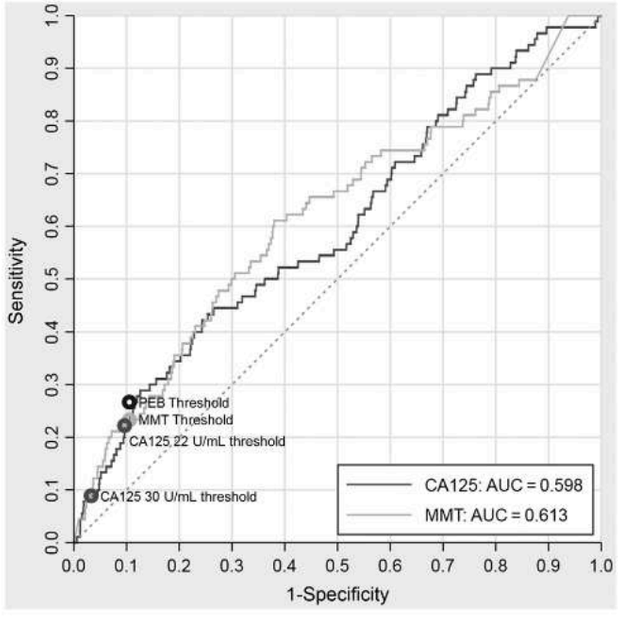

igure 2.
econdary analysis ROC curves for CA125 interpreted using MMT, threshold rules nd PEB for detection of iEOC/PPC cases. Circle points on the ROC curves give articular values of sensitivity and specificity provided by MMT and PEB orresponding to cutoff values obtained from the training set (MMT and PEB). bbreviations: PEB, parametric empirical Bayes; MMT, method of mean trends; A125, cancer antigen 125; AUC, area under roc-curve.

Longitudinal analysis of biomarkers

Method of Mean Trends

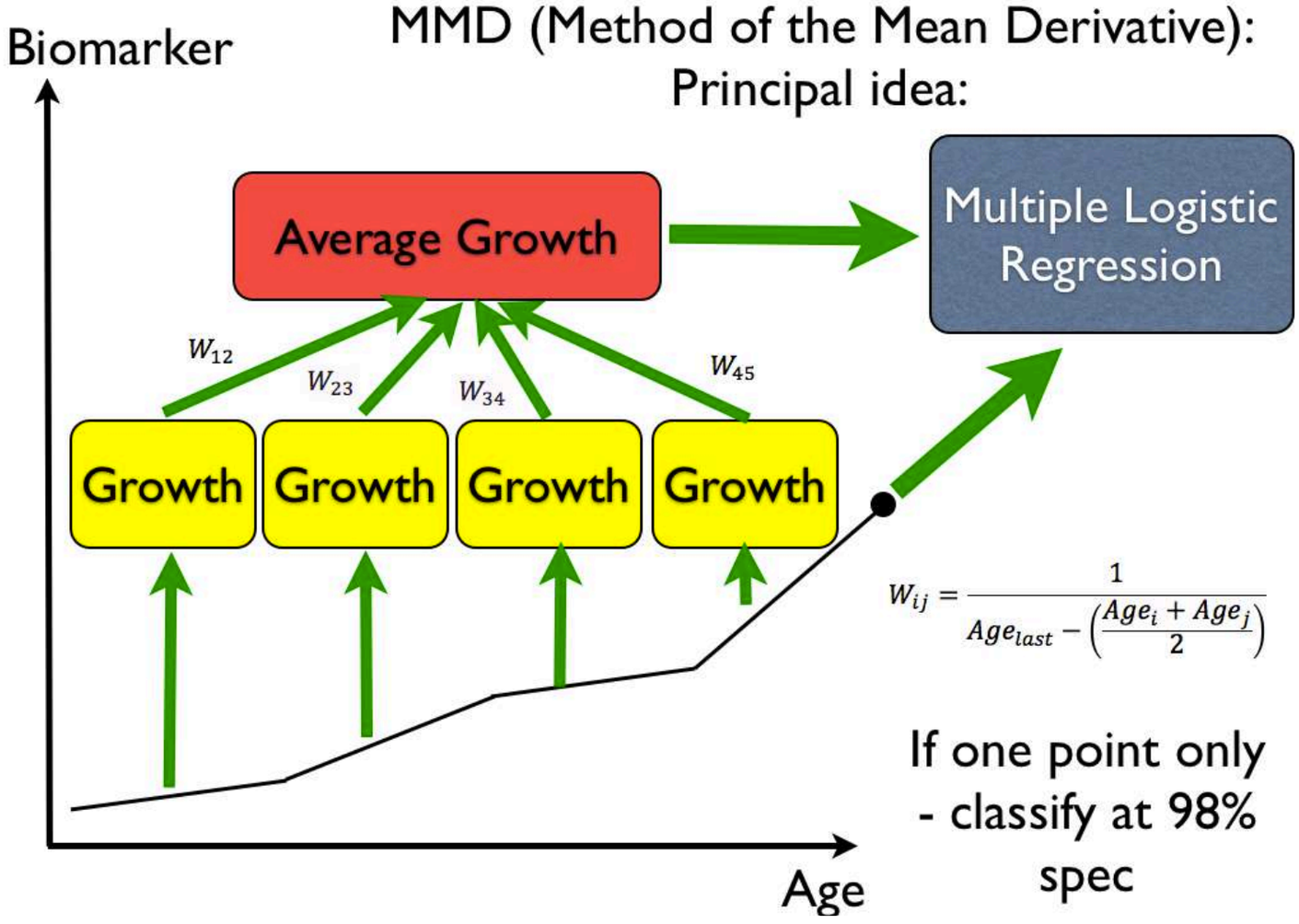

Comparison of longitudinal CA125 algorithms as a first line screen for ovarian cancer in the general population

Oleg Blyuss[1], Matthew Burnell[1], Andy Ryan[1], Aleksandra Gentry-Maharaj[1], Inés P. Mariño[1,2], Jatinderpal Kalsi[1], Ranjit Manchanda[1,6], John F. Timms[1], Mahesh Parmar[3], Steven J. Skates[4], Ian Jacobs[1,5,8], Alexey Zaikin[1,7*], and Usha Menon[1*].

Indicators used (for every i-th patient):

- Last measurement
- Trend 1 (Mean derivative)

$$\left(\sum_{j=1}^{k_i-1} \frac{y_{j+1}-y_j}{t_{j+1}-t_j} \frac{1}{t_{k_i}-(t_{j+1}+t_j)/2}\right)/(k_i-1)$$

- Trend 2

$$\left(\sum_{j=1}^{k_i-1} \frac{(y_{j+1}-y_j)(t_{j+1}-t_j)}{2}\right)/(k_i-1)$$

- Trend 3

$$\sqrt{\frac{\sum_{j=1}^{k_i}(y_j-\bar{y})^2}{k_i}}/\bar{y}$$

- Trend 4

$$\frac{\sum_{j=1}^{k_i} y_j t_j}{\sum_{j=1}^{k_i} t_j}$$

- Trend 5 (Variance)

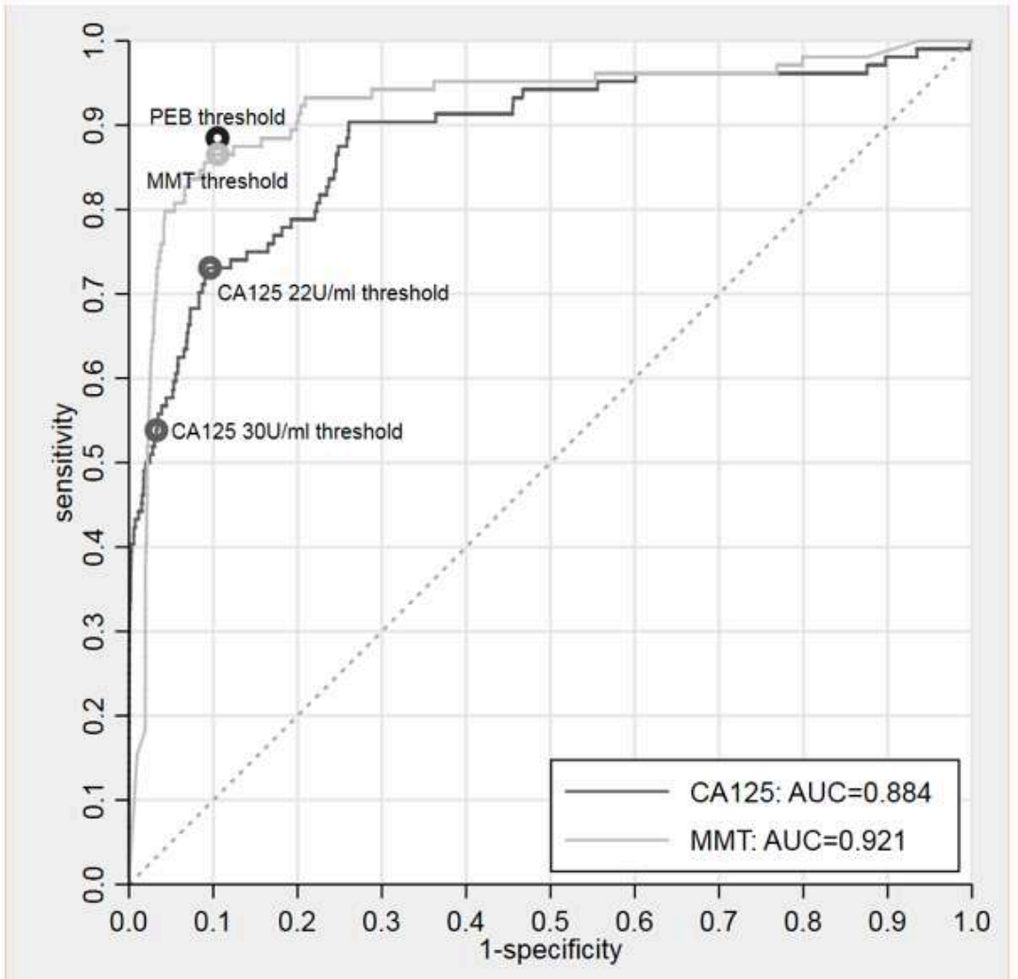

Approach I

Original dependences X1 and X2 on time

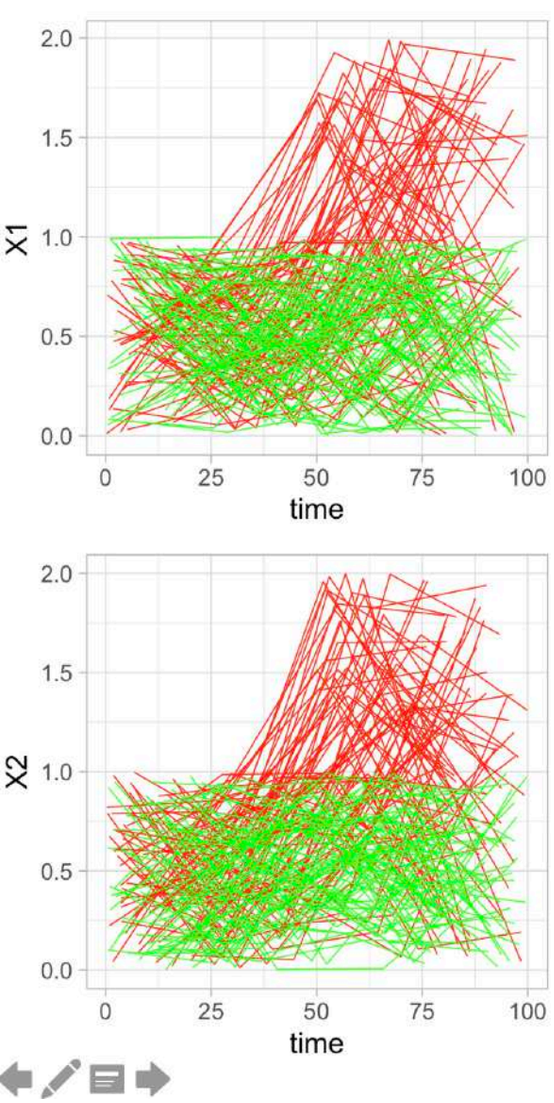

STEP I:

- considering each point as ***independent***;

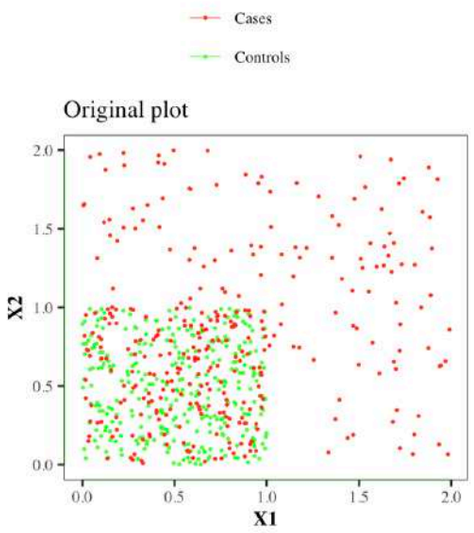

STEP II:

- building simple classification model (SVM, GLM, …) on X1 and X2;

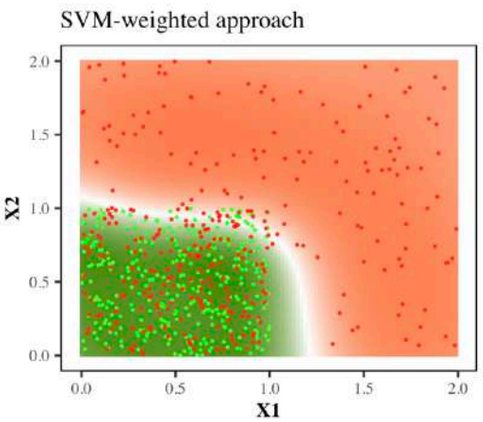

STEP III:

- get probabilities for each separate point and collect them to longitudinal vectors .

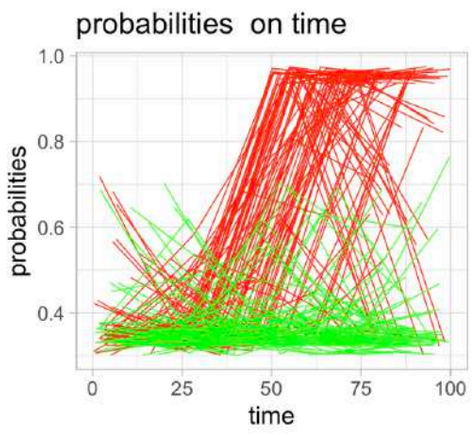

STEP IV:

- For each i sample calculating

A_i(P, time),
B_i(P, time),
C_i(P, time),
D_i(P, time) indices, where P – vector of probabilities

STEP V:

- Build classification model

M=M(A,B,C,D, score), where M – can be any of ML model (xgbTree, glmnet, nnet,…)

STEP VI;

- Use probabilities of M model as weights of edges between X1 and X2 vertices

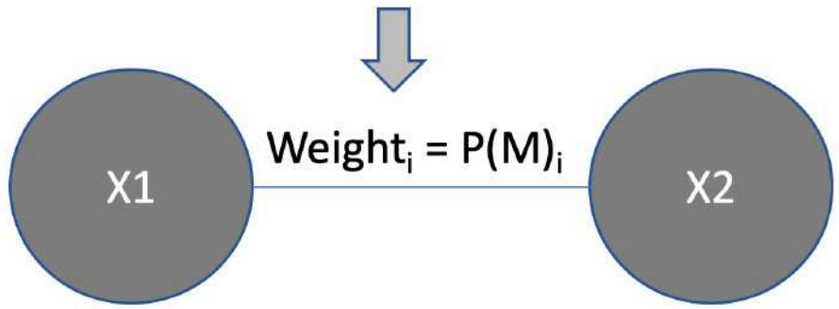

Approach II

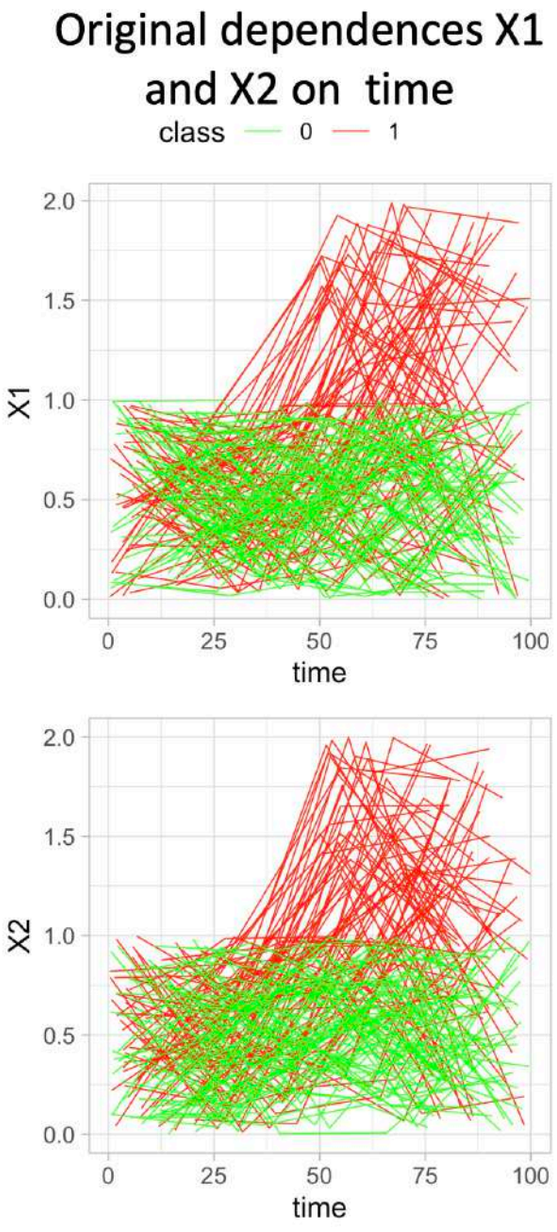

STEP I:

- For each i sample calculating

A_i^{X1}(X1, time), A_i^{X2}(X2, time),
B_i^{X1}(X1, time), B_i^{X2}(X2, time),
C_i^{X1}(X1, time), C_i^{X2}(X2, time),
D_i^{X1}(X1, time), D_i^{X2}(X2, time) indices;

STEP II:

- Build classification model

M=M(A^{X1},B^{X1},C^{X1},D^{X1},A^{X2},B^{X2},C^{X2},D^{X2},score), where M – can be any of ML model (xgbTree, glmnet, nnet,…)

STEP III:

- Use probabilities of M model as weights of edges between X1 and X2 vertices

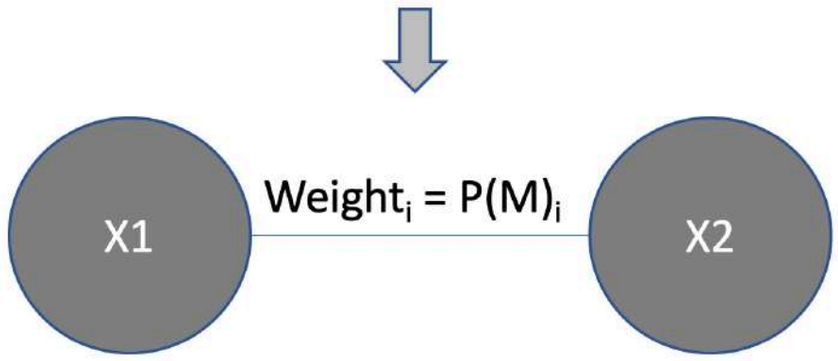

Combination with Graph Neural Networks

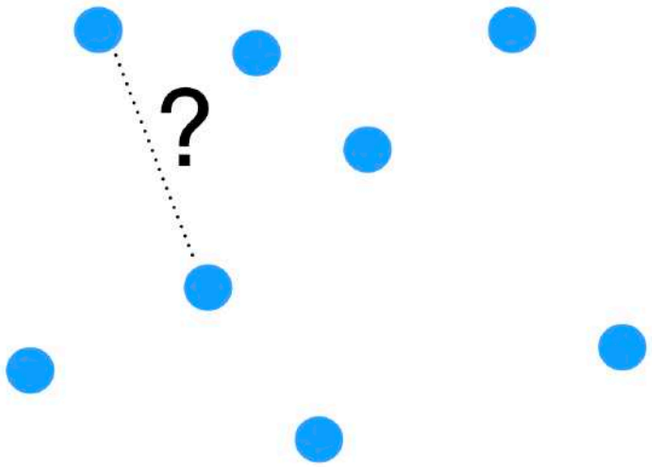

Neural Networks

?

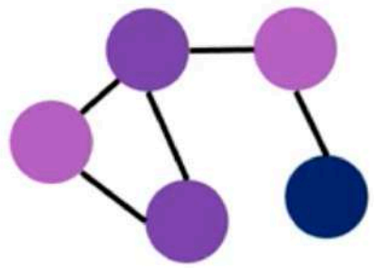

G = (V,E)

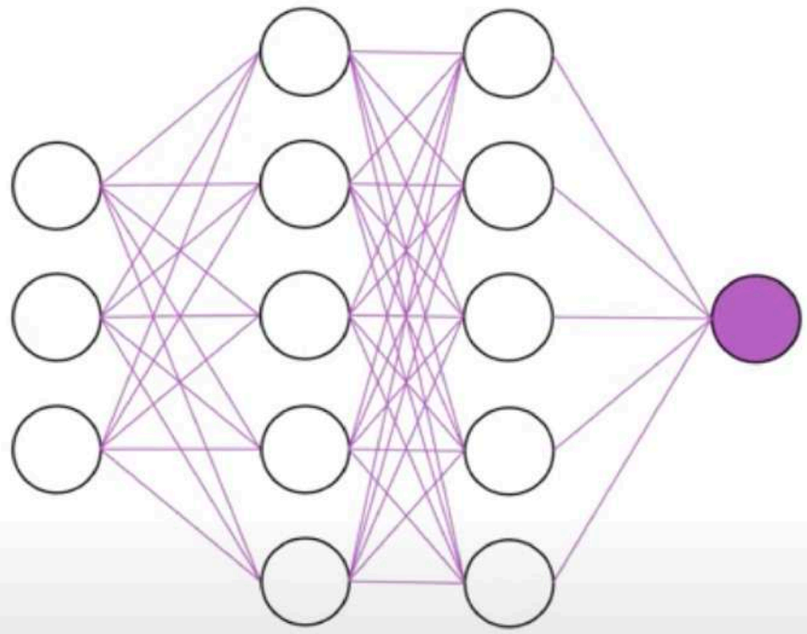

Combination with Graph Neural Networks

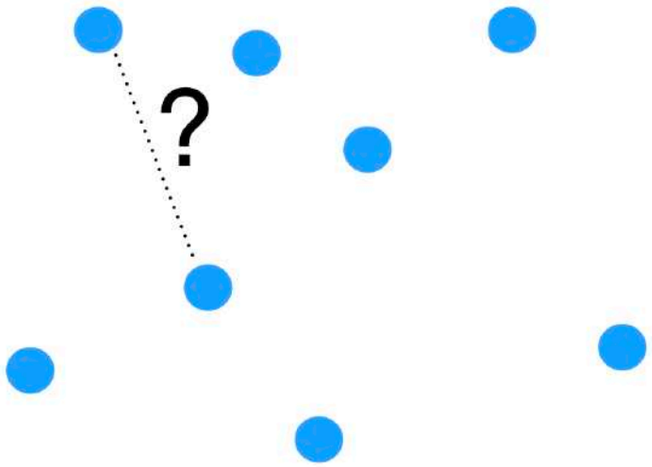

Neural Networks

Sample with R = 0.99

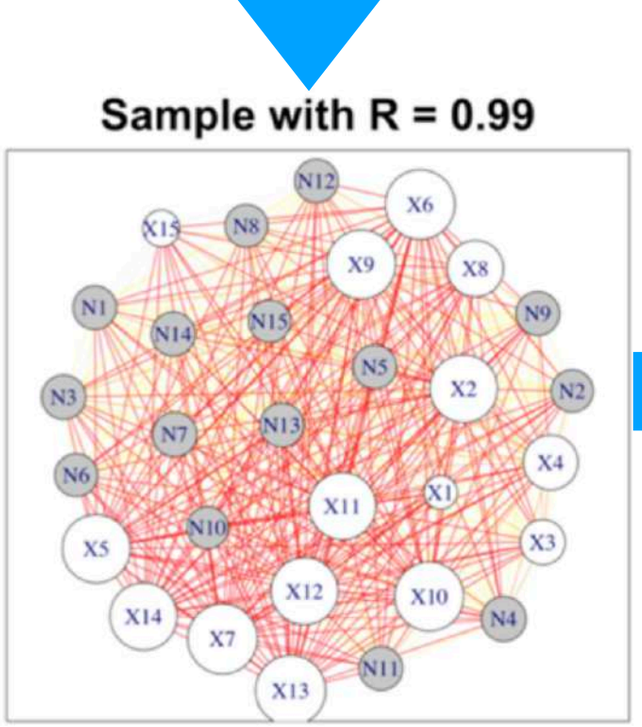

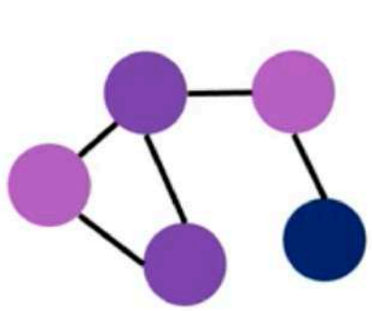

G = (V,E)

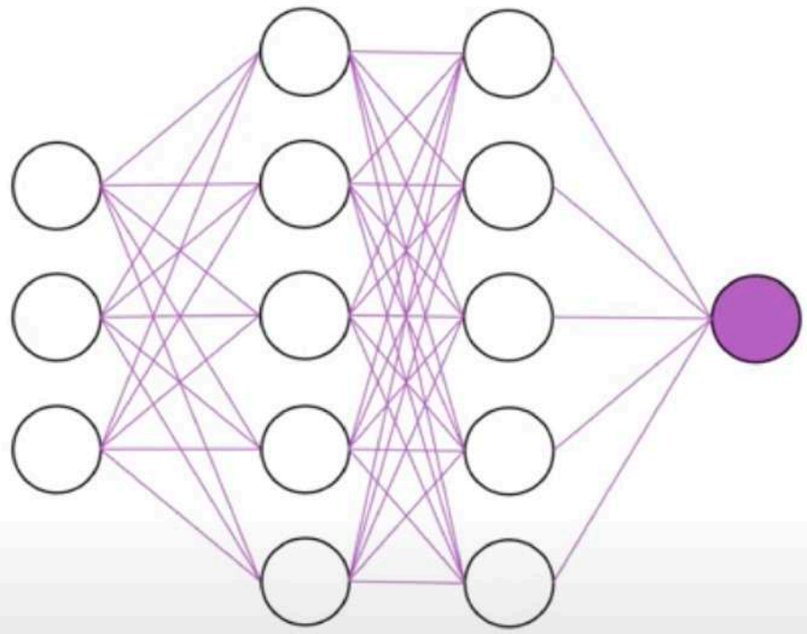

Comparison of the results of parenclitic approaches

The Graph Convolutional Network (GCN) vs ML models (glmnet, nnet, xgbTree), trained on the strengths of vertices on synthetic data

Color bars — confidence intervals of mean((AUCS TESTS of GCN) - (AUCS TESTS of model on Strengths))
Vertical black line in color bars – the mean
Color of bars, according to two-sided Paired Wilcoxon signed-rank test
Open circles – individual differences of mean

- NOT SIGNIFICANT, - SIGNIFICANT, GCN is better, - SIGNIFICANT, ML Model on Strengths is better

Ideal Spheres | zoomed figure | Broken Spheres | zoomed figure | Noisy Spheres | zoomed figure

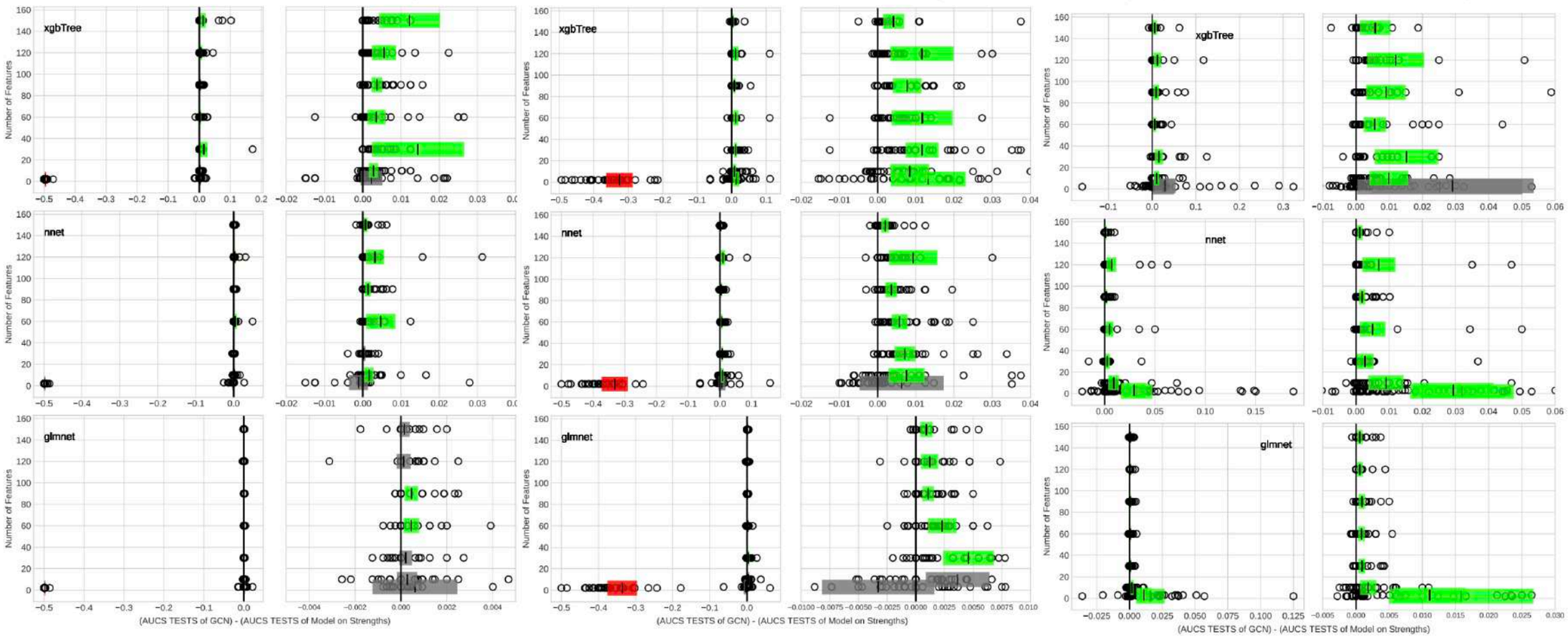

Network architecture

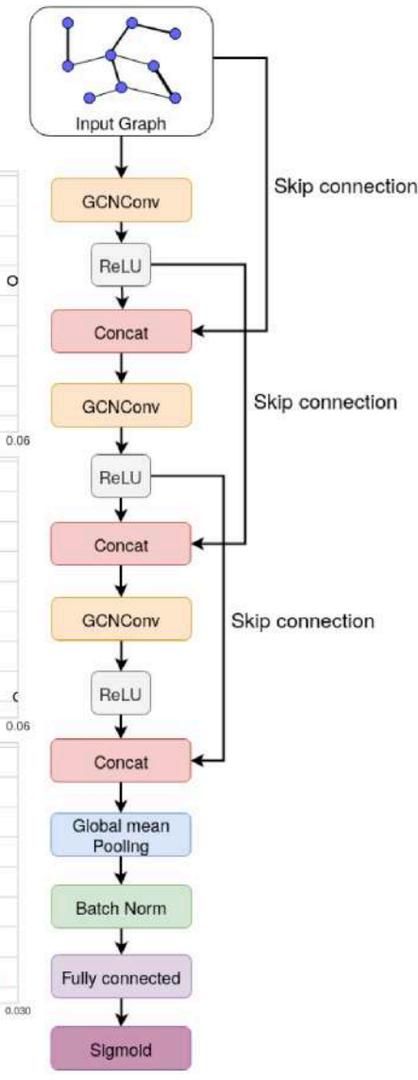

Tanya Nazarenko
Harry J. Whitwell
Oleg Blyuss
John F. Timms
Alexey Zaikin
Thomas Bartlett
Sofia Olhede
Usha Menon

Vadim Demichev

Markus Ralser lab
Clara Correia-Melo
Anja Freiwald
Oliver Lemke
Christoph Messner
Annika Röhl
Lukasz Szyrwiel
Spyros Vernardis
Matt White

Charité, Berlin

Florian Kurth group
Pinkus Tober-Lau
Charlotte Thibeault

Leif Sander group
Michael Mülleder group
Wolfgang Kübler group

Italy
Claudio Franceschi
Maria Julia Bacalini

Innsbruck
Ivan Tancevski group
Markus Keller group

NNGU
Misha Krivonosov
Misha Ivanchenko
Maria Vedunova

Spain
Ines Marino

Sechenov University
Vadim Ushakov
Alexander Suvorov

THANK YOU!!